https://doi.org/10.5194/egusphere-2025-5595
Preprint. Discussion started: 23 January 2026

Discovery of 2.45 Ga trondhjemitic gneiss in Eastern Hebei, North China Craton: A constraint on Precambrian crustal evolution

Jiahao Jing[1], Qian Liu[1], Yigui Han[1], Jinlong Yao[1], Donghai Zhang[1], Chenyang Sun[1], Jiakang Zheng[1], Guochun Zhao[2,1]

[1]State Key Laboratory of Continental Evolution and Early Life, NWU-HKU Joint Center of Earth and Planetary Sciences, Department of Geology, Northwest University, Xi'an 710069,
[2]Department of Earth and Planetary Sciences, The University of Hong Kong, Pokfulam Road, Hong Kong, China

Correspondence to: Qian Liu (liuqian@nwu.edu.cn)

Abstract. The early Paleoproterozoic era (2.45–2.20 Ga), known as the Tectono-Magmatic Lull (TML), is characterized by a decline in global magmatic activity. This study first identifies ca. 2.45 Ga trondhjemitic gneiss (2446 ± 15 Ma) in Eastern Hebei of the Eastern Block, North China Craton. These rocks exhibit adakitic geochemical characteristics, marked by high SiO_2, Al_2O_3, and Sr contents, with low MgO, Y, and Yb contents. Their low MgO, Cr, and Ni contents, along with slightly high zircon $\delta^{18}O$ (5.96–6.53 ‰) and positive $\varepsilon_{Hf}(t)$ (3.3–4.9) values, indicate that they originated from partial melting of a juvenile thickened lower crust. All samples show low concentrations of Y, Yb, Ti, Nb, and Ta, coupled with their high $(La/Yb)_N$ and Nb/Ta ratios, suggesting that they formed at a high-pressure condition, with garnet and rutile as residues. In combination with our new data and published zircon U-Pb ages in the region, we have identified multiple stages of magmatism (3.84–3.64 Ga, 3.53–3.22 Ga, 3.12–2.80 Ga, and 2.61–2.45 Ga) and metamorphism (3.50–3.23 Ga, 3.18–2.80 Ga, ~2.50 Ga, ~2.45 Ga, ~1.82 Ga) in Eastern Hebei. Based on a compilation of these magmatic zircon U-Pb ages and Hf isotope data, Eoarchean to early Paleoproterozoic crustal evolution processes in Eastern Hebei is established. The Eoarchean is dominated by Hadean crustal reworking, and the Paleoarchean is primarily characterized by crustal reworking with a minor contribution of crustal growth. Both crustal growth and reworking occurred during Mesoarchean time, with the proportion of crustal growth increasing from the Paleoarchean to the Mesoarchean. The late Neoarchean represents a major period of crustal growth with minor crustal reworking. The ca. 2.45 Ga trondhjemitic gneiss discovered in this study was probably a continuation of the late Neoarchean magmatism and the crustal growth persisted into this period.

https://doi.org/10.5194/egusphere-2025-5595
Preprint. Discussion started: 23 January 2026

1 Introduction

The early Paleoproterozoic era is a special period in Earth's history, during which a variety of fundamental paleoclimatic and tectono-magmatic changes occurred (Condie et al., 2009; Lyons et al., 2014; Zhai and Peng, 2020). On one hand, extensive paleoclimatic changes occurred in the early Paleoproterozoic, including a dramatic transition of atmosphere from oxygen-free to hypoxia-oxygenated (i.e., Great Oxidation Event), loss of mass-independent sulfur isotope fractionation, formation of largescale banded iron ore, significantly positive carbon isotope excursion, and development of widespread glaciations (i.e., Huronian glaciation) (Young, 2013; Eriksson and Condie, 2014; Partin et al., 2014; Condie et al., 2022). On the other hand, the global magmatic activity decreased dramatically between 2.45 and 2.2 Ga, as evidenced by a noticeable dip in light of global igneous and detrital zircon ages (Condie et al., 2009), with sporadic records of greenstone belt, tonalite-trondhjemite-granodiorite (TTG) suite, and large igneous provinces (LIPs) worldwide (Spencer et al., 2018; Wang et al., 2021; Yang et al., 2024). This interval of significantly reduced magmatic activity was named the "Tectono-Magmatic Lull (TML)" (Partin et al., 2014; Teixeira et al., 2015; Spencer et al., 2018). Some scholars proposed that the TML was related to the global plate tectonic shutdown and continental crust growth was stagnated during the TML (O'Neill et al., 2007; Condie et al., 2009; Spencer et al., 2018).

However, some recent studies have revealed that the TML might not have been completely quiet, as many early Paleoproterozoic magmatic activities have been reported in different cratons (Partin et al., 2014). For example, the early Paleoproterozoic mafic dike swarms are well-documented globally, including the ~2.34 Ga diabase dike swarms in the Karelian Craton (Stepanova et al., 2015), the ~2.36 Ga Bangalore gabbro-diabase dike swarms in the Dharwar Craton (Halls et al., 2007; Kumar et al., 2012; Söderlund et al., 2019; Ramesh et al., 2020), the ~2.42 Ga Widgiemooltha-Binneringie dike swarms in the Yilgarn Craton (French et al., 2002; Wingate, 2017; Siégel et al., 2024, and the 2.42–2.37 Ga Scourie dike swarms in the North Atlantic Craton (Davies and Heaman., 2014; Zakharov et al., 2019). In addition, the 2.43–2.20 Ga silicic magmatic rocks, including TTG suites and calc-alkaline granitoids, have been reported in the Arrowsmith Orogenic Belt of the Rae Craton (Hartlaub, et al., 2007; Neil et al., 2025), the Minerio Orogenic Belt of the San Francisco Craton (Teixeira et al., 2015; Alkmim et al., 2017), and the Trans-North China Orogen (TNCO) of the North China Craton (NCC) (Diwu et al., 2014; Zhou et al., 2021, 2024; Zhou and Zhai., 2022; Wang and Long, 2024). Accordingly, some scholars have suggested that plate tectonics and crustal growth persisted throughout the TML and attributed the lack of the early Paleoproterozoic magmatic records to preservation bias (Partin et al., 2014; Pehrsson et al., 2014; Yang and Santosh, 2015).

As one of the globally typical area for the early Paleoproterozoic magmatism, several magmatic activities during the TML have been discovered in the TNCO, Kondalite Belt, and Jiao-Liao-Ji Belt of the NCC, with various rock types of gabbro, diorite, TTG gneiss, and granitoid gneiss (Diwu et al., 2014; Du et al., 2016; Duan et al., 2021; Zhou et al., 2021, 2024; Wang et al., 2021; Zheng et al., 2022; Zhou and Zhai, 2022; Wang and Long, 2024). However, few early Paleoproterozoic magmatic records were found in the Western and Eastern blocks of the NCC. In this study, we firstly identify the 2.45 Ga trondjemitic gneiss in Eastern Hebei and conduct an integrated study of petrology, whole-rock geochemistry, and zircon U-Pb dating and

https://doi.org/10.5194/egusphere-2025-5595
Preprint. Discussion started: 23 January 2026

Hf-O isotope compositions. These new data, along with previously published data in Eastern Hebei, allow us to establish the geochronological framework of the Precambrian basement in this region, which provides insights into the Archaean to early Paleoproterozoic crustal evolution history.

2 Geological setting and samples

As the largest and oldest craton in China, the NCC is tectonically bounded by the Central Asian Orogenic Belt to the north, the Qinling-Dabie Orogenic Belt to the south, and the Qilian Orogenic Belt to the west (Fig. 1, Zhao et al., 2005). It consists mainly of Archean-Paleoproterozoic basement and unmetamorphosed Paleoproterozoic-Mesozoic sedimentary cover (Zhao et al., 2005; Geng et al., 2012; Zhao and Zhai, 2013). The basement of the NCC is subdivided into the Eastern Block and the Western Block, which were amalgamated in the Paleoproterozoic (ca. 1.85 Ga) along the TNCO (Zhao et al., 2005). The Western Block was amalgamated by the Yinshan and Ordos blocks along the Khondalite Belt at ∼1.95 Ga, while the Eastern Block was formed at ∼1.90 Ga by collision of the Longgang and Langrim blocks along the Jiao-Liao-Ji Belt (Zhao et al., 2005).

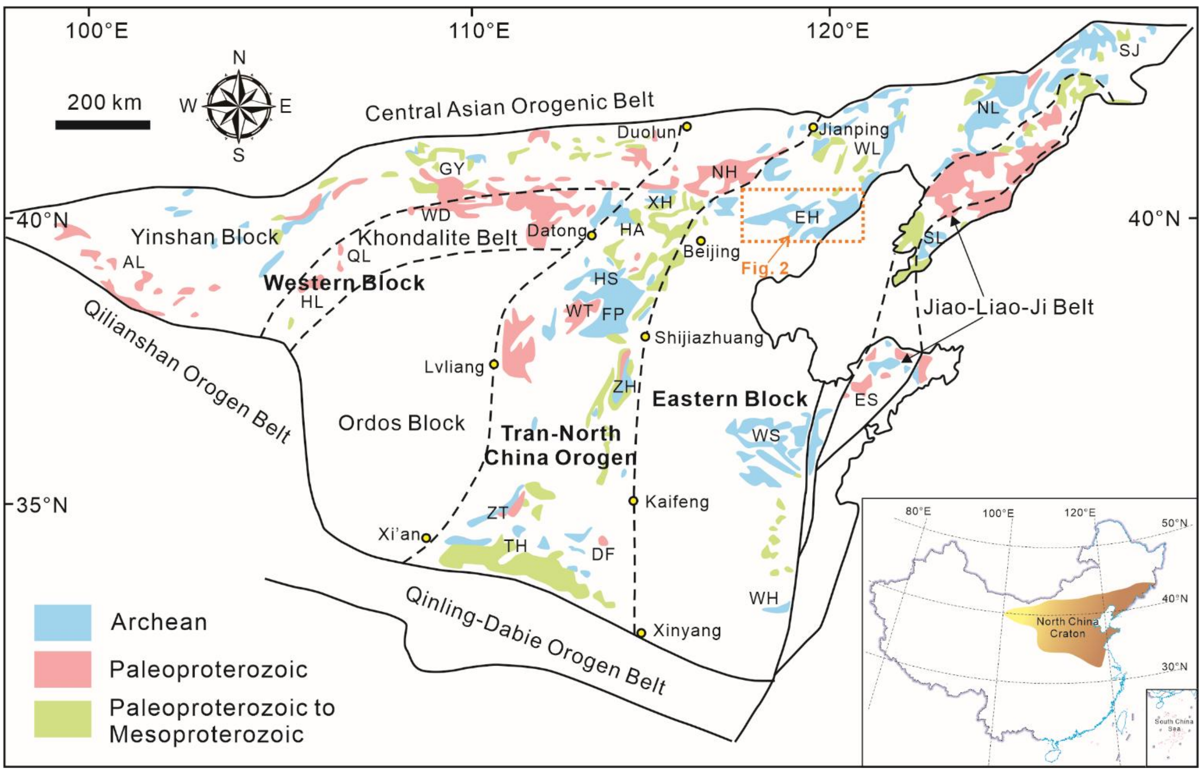

Figure 1: Simplified geological map of the North China Craton showing its major tectonic units and the distribution of Precambrian basement (modified after Zhao et al., 2005). Abbreviations of terranes: AL–Alxa, GY–Guyang, WD–Wulashan-Daqingshan, QL–Qilian, HL–Helanshan, NH–Northern Hebei, XH–Xuanhua, HA–Huai'an, HS–Hengshan, WT–Wutai, FP–Fuping, ZH–Zanhuang, ZT–Zhongtiao, TH–Taihua, DF–Dengfeng, WL–Western Liaoning, NL–Northern Liaoning, SJ–Southern Jilin, EH–Eastern Hebei, WS–Western Shandong, WH–Wuhe, ES–Eastern Shandong, and SL– South Liaoning.

https://doi.org/10.5194/egusphere-2025-5595
Preprint. Discussion started: 23 January 2026

Located in the western margin of the Eastern Block, Eastern Hebei is a classic region where the Archean basement is widely exposed (Zhao et al., 2005; Geng et al., 2006). A variety of rock types have been recognized in this area, including TTG gneisses, dioritic gneisses, charnockites, potassic granites, supracrustal rocks, and small amounts of metabasic dykes (Yang et al., 2008; Nutman et al., 2011; Bai et al., 2014, 2015, 2019; Duan et al., 2017, 2022; Fu et al., 2016, 2017; Li et al., 2024). The supracrustal rocks show typical features of the Archean greenschist belt, and consist of metasedimentary and metabasic rocks with a few Banded Iron Formations and ultramafic interlayers (Geng et al., 2006; Polat et al., 2006; Guo et al., 2013, 2014, 2015, 2017; Wang et al., 2019a; Li et al., 2024). The Archean rock types in Eastern Hebei show spatial variations and are divided into five litho-tectonic units: (I) the Saheqiao linear-structural belt, (II) the Taipingzhai ovate-structural domain, (III) the Qian'an gneiss dome, (IV) the Lulong-Shuangshanzi supracrustal rock belt, and (V) the Anziling gneiss dome (Fig. 2, Wei, 2018). In addition, the Archean rocks in Eastern Hebei experienced intensive metamorphism and deformation. They are characterized by Archean unique dome-and-keel structures, with the supracrustal rocks (the Lulong-Shuangshanzi supracrustal belt) occurring as keels in the TTG gneiss domes (the Anziling gneiss dome) (Liu and Wei, 2018; Zhao et al., 2021). The degrees of metamorphism of these rocks also show spatial variations. The rocks in the western segment experienced upper amphibolite- to granulite-facies metamorphism, whereas the eastern rocks underwent greenschist- to amphibolite-facies metamorphism (Yang and Wei, 2017a, b; Liu and Wei, 2018; Duan et al., 2019; Liu et al., 2020, 2022).

Most of the TTG and granitoid gneisses in Eastern Hebei show magmatic crystallization ages of 2.58–2.49 Ga and metamorphic ages of 2.53–2.31 Ga (Geng et al., 2006; Yang et al., 2008; Nutman et al., 2011; Bai et al., 2014, 2016; Fu et al., 2016; Yao et al., 2017; Li et al., 2019; Duan et al., 2022; Zhao et al., 2025a). In addition, some Eoarchean to Mesoarchean granitoids (3.80–2.90 Ga) have been identified in the Huangbaiyu, Labashan, Caochang, and Caozhuang areas of Eastern Hebei (Nutman et al., 2011; Sun et al., 2016; Fu et al., 2019; Liou et al., 2019; Liou and Guo, 2019a; Wan et al, 2021, 2023; Dong et al., 2024, 2025; Zhao et al., 2025b). The supracrustal rocks have primary protolith deposition and magmatic ages of 2.61–2.50 Ga (Zhang et al., 2012; Guo et al., 2013, 2014; 2015, 2017; Fu et al., 2016; Duan et al., 2017; Lu et al., 2017; Liu and Wei, 2020; Duan et al., 2022). Notably, the Palaeoarchaean (3.45 Ga) and Mesoarchean (3.1–2.9 Ga) ultramafic-mafic rocks were also reported in Labashan, Longwan, and Caochang areas of Eastern Hebei (Liou et al., 2019; Wang et al., 2019a; Dong et al., 2025). The supracrustal rocks yield two groups of metamorphic ages at 2.53–2.47 Ga and 1.97–1.80 Ga (Duan et al., 2017, 2022; Yang and Wei, 2017a, b; Lu and Wei, 2020).

https://doi.org/10.5194/egusphere-2025-5595
Preprint. Discussion started: 23 January 2026

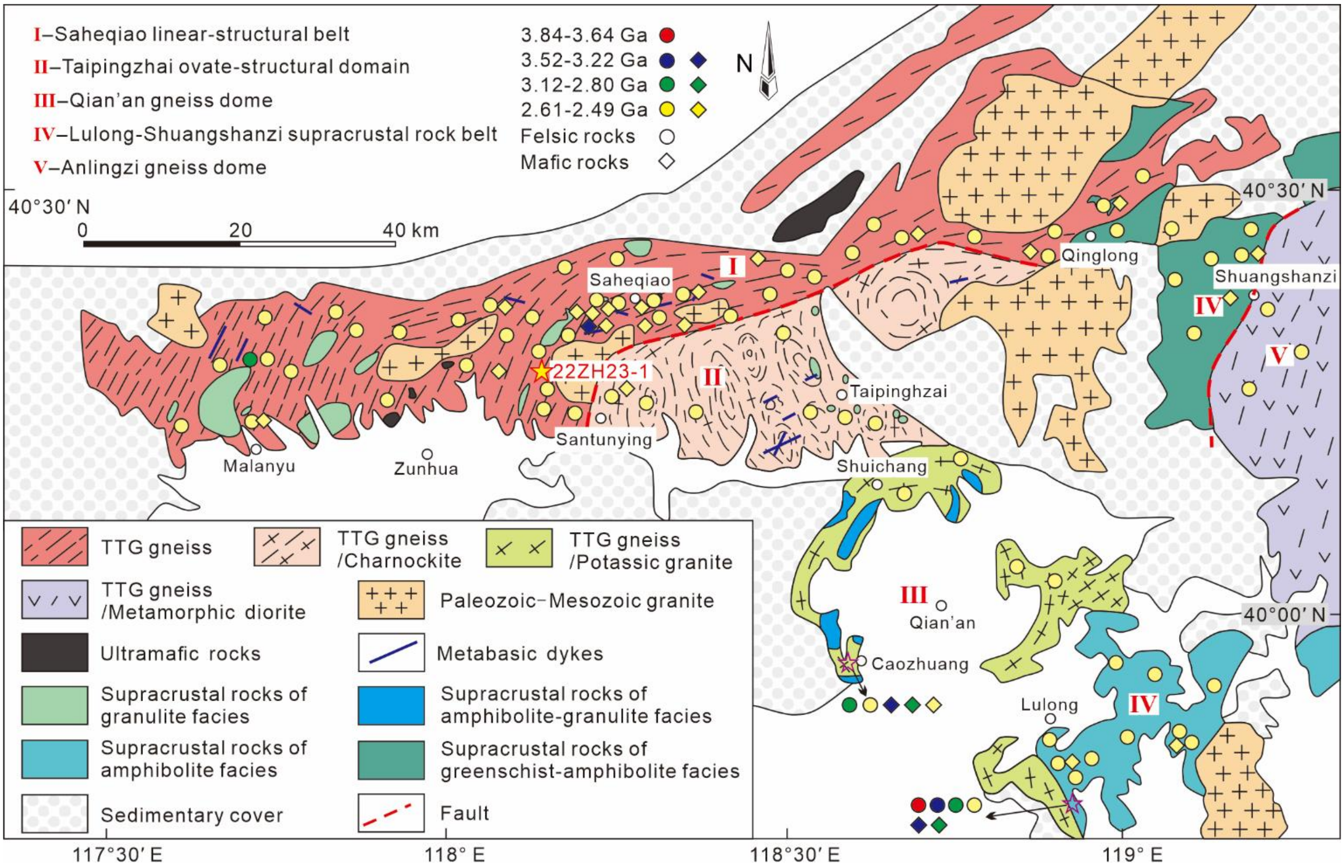

Figure 2: Simplified geological map of Eastern Hebei showing sampling locations (modified after Jing et al., 2025). The data of the felsic and mafic rocks are shown in Supplementary Table S1.

The 2.45 Ga trondhjemitic gneiss in this study was discovered on the road to Qiuhuayu Village (GPS: N 40°15′38.47″, E 118°07′25.84″). In the field, these rocks are grayish-white and display gneissic structures (Fig. 3a, b). They are medium- to coarse-grained and composed primarily of plagioclase (45–55 %) and quartz (40–45 %), with minor alkali-feldspar, clinopyroxene, and accessory minerals such as magnetite (<5 %) (Fig. 3c, d). Quartz occurs as small grains that fill the interstitial spaces between larger plagioclase crystals (Fig. 3c, d).

https://doi.org/10.5194/egusphere-2025-5595
Preprint. Discussion started: 23 January 2026

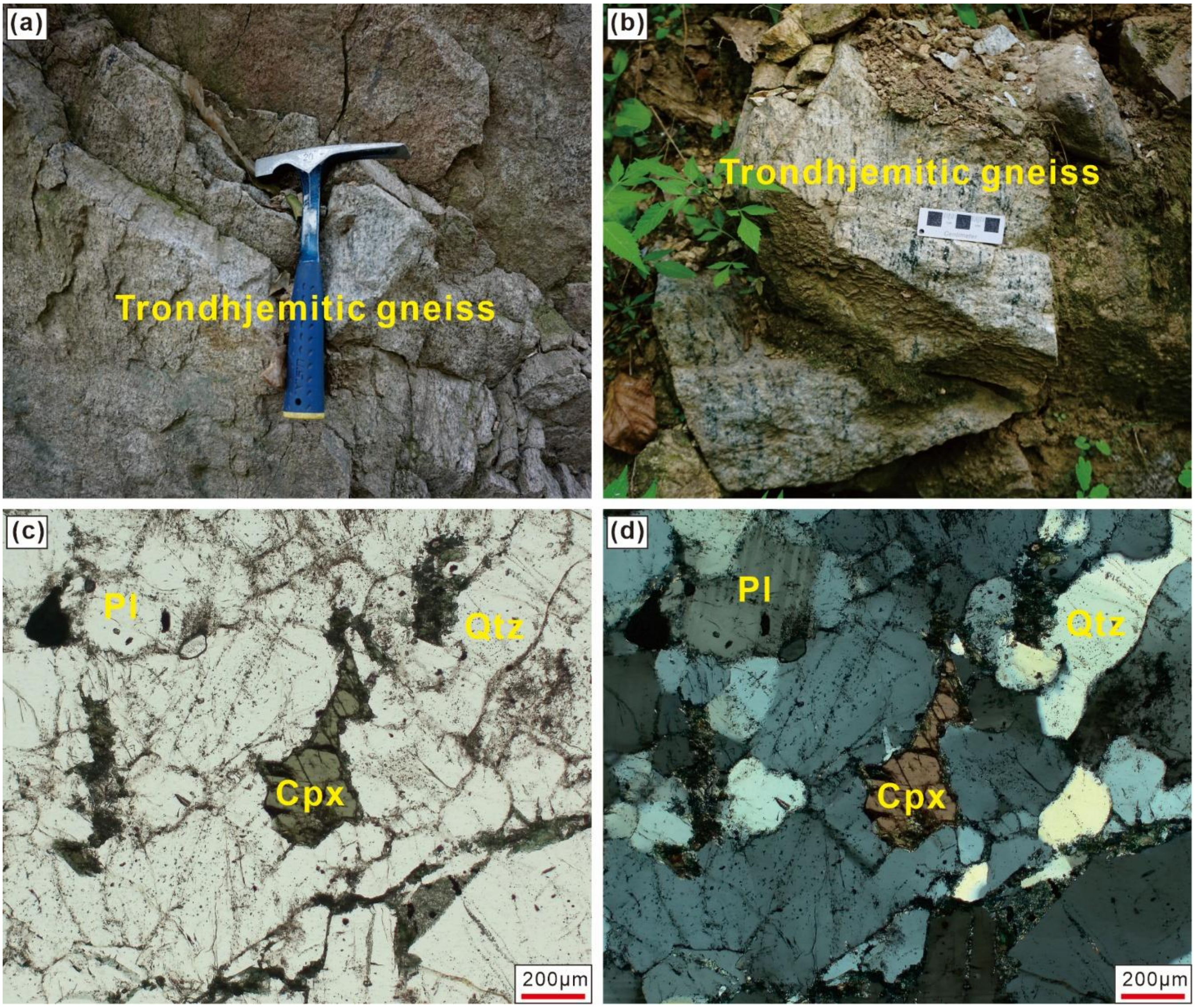

Figure 3: Representative field photographs and microphotographs of the 2.45 Ga trondhjemitic geniss in Eastern Hebei. Mineral abbreviations: Qtz–quartz, Pl–plagioclase, and Cpx–clinopyroxene.

3 Analytical methods

3.1 Zircon U-Pb dating

Zircons U-Pb dating used instruments of Agilent 7700x quadrupole inductively coupled plasma mass spectrometry system (ICP-MS) equipped with a 193 nm ArF excimer laser ablation system (LA) at FocuMS Technology Co., Ltd., Nanjing, China. The operating conditions include an analysis spot diameter of 33 μm, a repetition rate of 6 Hz, and an energy density of 4.5 J/cm^2. Zircon standard 91500 (Wiedenbeck et al., 1995) was used to calibrate U-Pb isotopic ratios, and two zircon standards

https://doi.org/10.5194/egusphere-2025-5595
Preprint. Discussion started: 23 January 2026

(GJ-1 and TANZ) were analyzed after every eight sample spots. The analysed zircons 91500, GJ-1, and TANZ yielded weighted mean $^{206}Pb/^{238}U$ ages of 1062.4 ± 1.2 Ma, 603.8 ± 2.1 Ma, and 565.7 ± 1.8 Ma, respectively, which agree well with their recommended ages (Sláma et al., 2008; Wiedenbeck et al., 1995). Raw data was processed by using ICPMSDataCal (Liu et al., 2010). Age calculation and plotting were conducted by applying Isoplot (ver. 4.00; Ludwig, 2003).

3.2 Whole-rock major and trace elemental analyses

Whole-rock major and trace elemental analyses were conducted at FocuMS Technology Co., Ltd., Nanjing, China. Major elements were analyzed using an Agilent 5110 inductively coupled plasma-optical emission spectroscopy (ICP-OES; Penang, Malaysia), while trace elements were analyzed using an Agilent 7700x quadrupole ICP-MS (Tokyo, Japan). The analytical accuracy is generally < 5 % for major elements and < 10 % for most trace elements.

3.3 Zircon Lu-Hf isotopic analyses

In-situ zircon Lu-Hf isotope analysis was conducted using a *Nu Plasma II* multiple collector (MC) ICP-MS equipped with a RESOlution-LR 193 nm ArF excimer laser at FocuMS Technology Co., Ltd., Nanjing, China. Analyses were performed with a laser beam diameter of 50 μm, a repetition rate of 9 Hz, and an ablation time of 40 s. Three of six standard zircons (TANZ, 91500, GJ-1, Plešovice, Mud Tank, and Penglai) were analyzed after every fifteen samples to monitor the instrument's reliability and stability. The measured $^{176}Hf/^{177}Hf$ ratios of TANZ (0.281819 ± 0.000003), 91500 (0.282308 ± 0.000003), GJ-1 (0.282004 ± 0.000007), Plešovice (0.282489 ± 0.000004), Mud Tank (0.282510 ± 0.000007), and Penglai (0.282906 ± 0.000006) were consistent with the recommended values within the error range (TANZ = 0.281821 ± 0.000042, Hu et al., 2021, 91500 = 0.282309 ± 0.000004, Yuan et al., 2008; GJ-1 = 0.282013 ± 0.000009, Yuan et al., 2008; Plešovice = 0.282482 ± 0.000013, Slámaet al., 2008; Mud Tank = 0.282513 ± 0.000006, Yuan et al., 2008; Penglai =0.282906 ± 0.000010, Li et al., 2010). Zircon $\varepsilon_{Hf}(t)$ values were calculated based on present-day chondritic ratios ($^{176}Hf/^{177}Hf$ = 0.282785, $^{176}Lu/^{177}Hf$ = 0.0336; Bouvier et al., 2008) and ^{176}Lu decay constant ($\lambda^{176}Lu = 1.867 \times 10^{-11}$; Söderlund et al., 2004). For calculating two-stage Hf model ages (T_{DM2}), a $^{176}Lu/^{177}Hf$ ratio for average continental crust is 0.015 (Griffin et al., 2002), with respect to depleted mantle with a present-day $^{176}Hf/^{177}Hf$ ratio of 0.28325 and a $^{176}Lu/^{177}Hf$ ratio of 0.0384 (Griffin et al., 2000).

3.4 Zircon O isotopic analyses

In situ zircon oxygen isotopes were analyzed using the CAMECA IMS-1300HR3 ion microprobe in the multi-collection mode at the State Key Laboratory of Critical Earth Material Cycling and Mineral Deposits, Nanjing University. The $^{133}Cs^{+}$ primary ion beam was accelerated at 12kV, with an intensity of ~2.6 nA and an analytical spot of 20 μm. Oxygen isotopes were measured in multi-collector mode using two off-axis Faraday cups. The measured oxygen isotopic data was normalized to Vienna Standard Mean Ocean Water compositions (VSMOW, $^{18}O/^{16}O$ = 0.0020052; Rehman et al., 2018) and corrected for instrumental mass fractionation (IMF) using the Penglai zircon standard ($\delta^{18}O_{VSMOW}$ = 5.31±0.1 ‰, Li et al., 2010). The Qinghu

https://doi.org/10.5194/egusphere-2025-5595
Preprint. Discussion started: 23 January 2026

zircon was used as a secondary zircon standard, and two measurements yielded a weighted mean value of 5.47 ± 0.04 ‰ (*n* = 2), consistent with the recommended value of 5.4 ± 0.2 ‰ (Li et al., 2013).

4 Analytical results

4.1 Zircon U-Pb ages

Zircon grains from sample 22ZH23-1 are subhedral to euhedral, with a length of 100 to 300 µm and aspect ratios of 1:1 to 3:1 (Fig. 4a). Most of the zircon grains show clear oscillatory zoning in cathodoluminescence (CL) images and possess high Th/U ratios, along with their steep chondrite-normalized REE patterns, indicating a magmatic origin (Fig. 4b). In addition, some zircon grains are featured by core-rim textures, with oscillatory magmatic cores and bright structureless metamorphic rims. Nonetheless, the rims are too narrow to be analyzed.

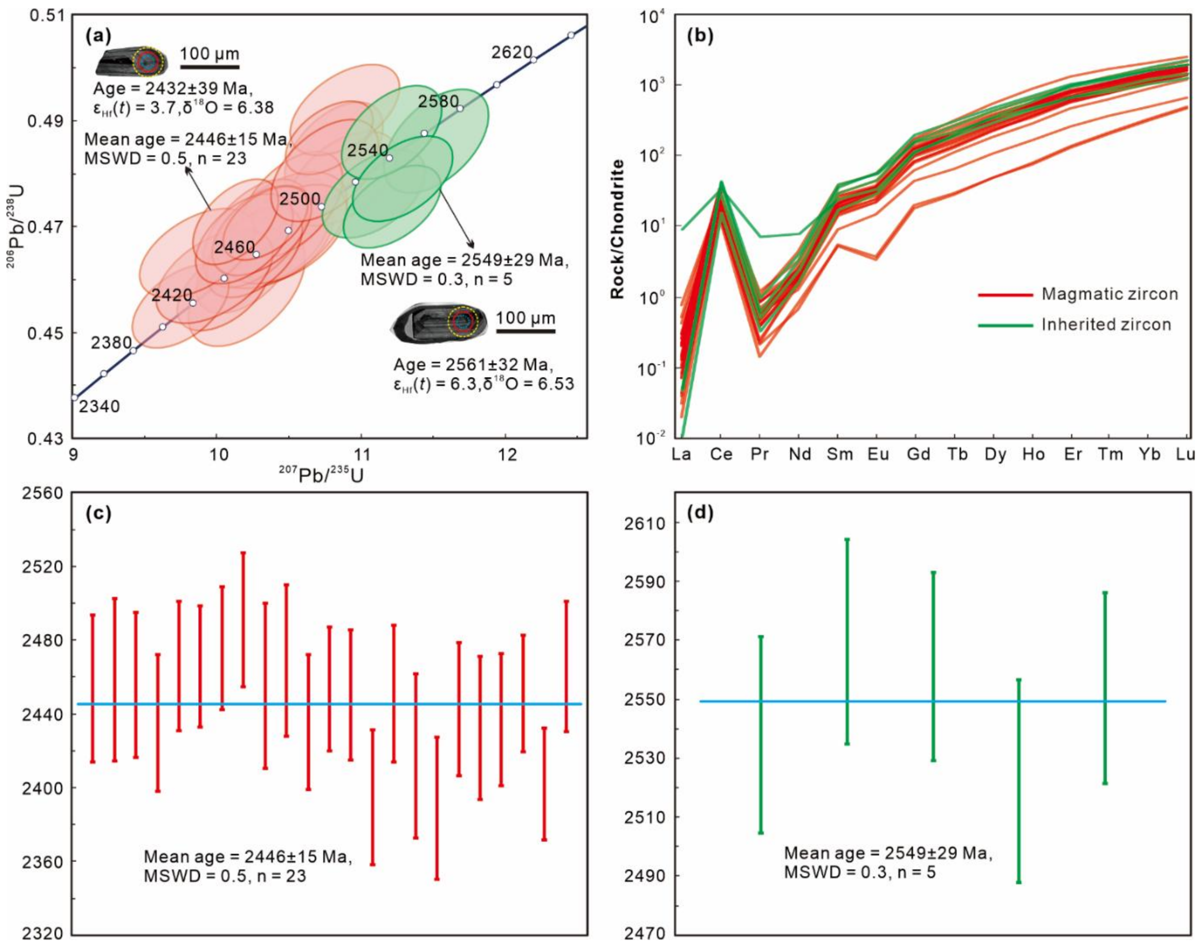

Figure 4: Zircon U-Pb concordia diagram and representative zircon cathodoluminescence images (a), chondrite-normalized zircon REE patterns (b), weighted mean age of the magmatic zircons (c), and weighted mean age of the inherited zircons (d) of the trondhjemitic geniss.

https://doi.org/10.5194/egusphere-2025-5595
Preprint. Discussion started: 23 January 2026

A total of 30 analyses were conducted on zircon cores of sample 22ZH23-1, and two analyses were excluded from calculation due to their high discordance (> 5 %). Detailed LA-ICP-MS zircon U-Pb dating results and rare earth element (REE) concentrations are presented in Supplementary Tables S2 and S3, respectively. The remaining 28 analyses yield apparent $^{207}Pb/^{206}Pb$ ages ranging from 2569 to 2389 Ma and contain two age populations (Fig. 4a). (1) 23 analyses define a $^{207}Pb/^{206}Pb$ weighted mean age of 2446 ± 15 Ma (mean square of weighted deviates, MSWD = 0.5), which is interpreted as the crystallization age of the protolith of this sample (Fig. 4c). (2) 5 analyses give an older $^{207}Pb/^{206}Pb$ weighted mean age of 2549 ± 29 Ma (MSWD = 0.3), which may represent the crystallization age of inherited zircons (Fig. 4d). These zircon grains were either reintroduced into late-phased magmatic sources or entrained during magma transport.

4.2 Whole-rock major and trace element compositions

Four samples were selected for whole-rock major and trace element composition analyses, and the results are shown in Supplementary Table S4. All samples have high concentrations of SiO_2 (66.99–69.89 wt.%) and Al_2O_3 (16.64–18.30 wt.%). They are enriched in Na_2O (6.27–6.84 wt.%) but depleted in K_2O (0.45–0.91 wt.%) contents, leading to high Na_2O/K_2O ratios of 6.96–15.21. These samples show low concentrations of $Fe_2O_3^T$ (1.53–1.76 wt.%) and MgO (0.44–0.58 wt.%), with $Mg^\#$ values of 36–42. All samples plot within the granodiorite field in the total alkali-silica (TAS) diagram (Fig. 5a) and belong to the low-K tholeiitic series in the K_2O vs. SiO_2 diagram (Fig. 5b). They yield A/CNK [molar ratio of $Al_2O_3/(CaO+Na_2O+K_2O)$] ratios of 0.98–1.01, indicating metaluminous to weakly peraluminous characteristics (Fig. 5c). Further classification on the anorthite-albite-orthoclase (An-Ab-Or) diagram reveals that they belong to trondhjemite (Fig. 5d).

https://doi.org/10.5194/egusphere-2025-5595
Preprint. Discussion started: 23 January 2026

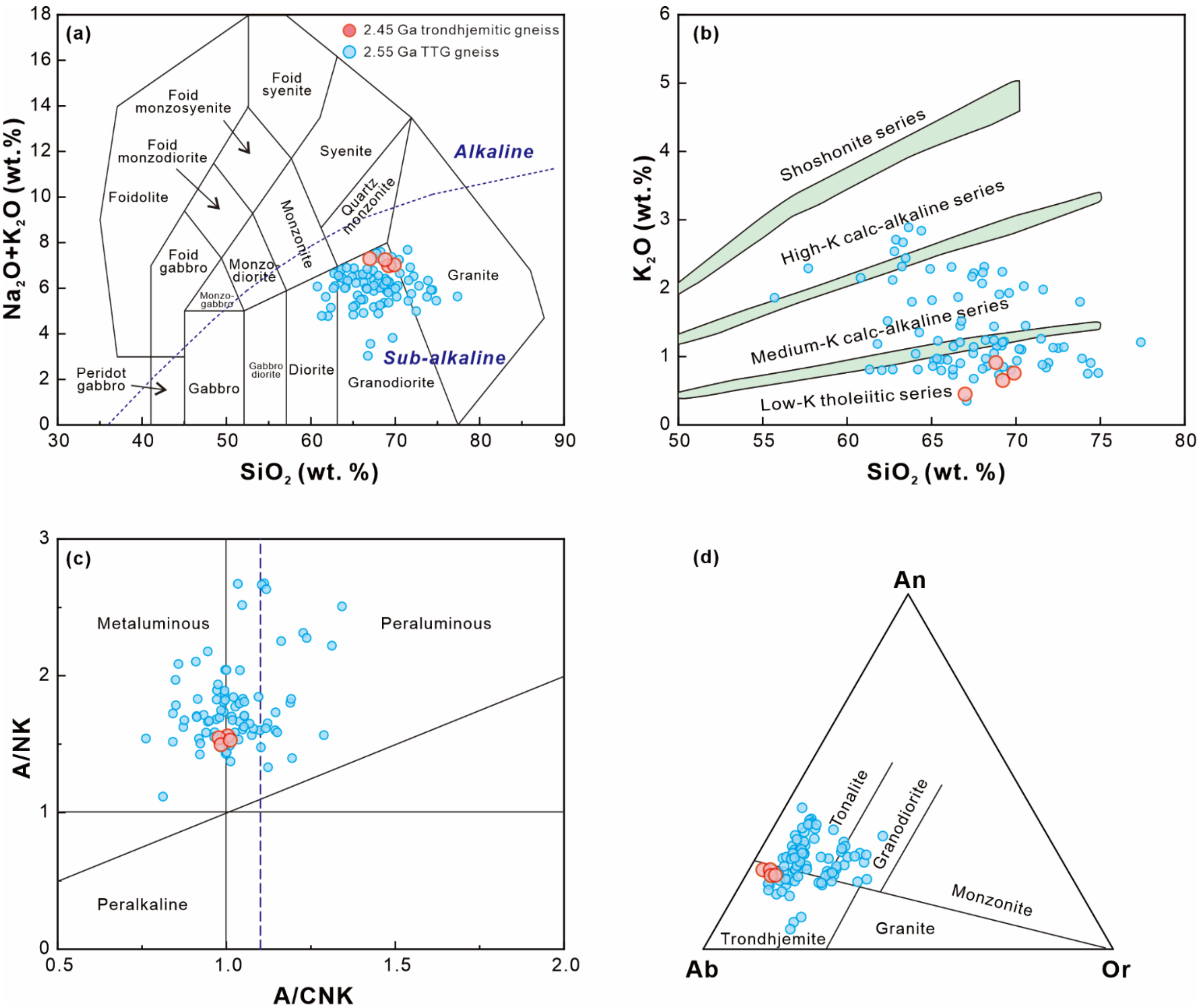

Figure 5: Geochemical classification of the trondhjemitic geniss samples. (a) Total alkali vs silica (TAS) diagram (after Middlemost, 1994); (b) K_2O vs. SiO_2 diagram (after Peccerillo and Taylor, 1976); (c) A/NK [Al_2O_3/ (Na_2O + K_2O)] vs. A/CNK [Al_2O_3/ (CaO + Na_2O + K_2O)] (after Maniar and Piccoli, 1989). (d) Feldspar An-Ab-Or classification diagram (after Barker, 1979). The data of the 2.55 Ga TTG gneiss are from Yang et al., 2008; Nutman et al., 2011; Bai et al., 2014, 2016; Fu et al., 2016; Li et al., 2019; Jing et al., 2025; Zhao et al., 2025a.

These samples contain total rare earth element (REE) contents ranging from 19.3 to 27.5 ppm. They are characterized by enrichments in light rare earth elements (LREEs) but depletions of heavy rare earth elements (HREEs), with $(La/Yb)_N$ ratios of 28.3–38.9 (Fig. 6a). In addition, they exhibit significantly positive Eu anomalies (δEu = 1.73–2.34) and slight Ce anomalies (δCe = 0.93–1.01) (Fig. 6a). All samples have high concentrations of Sr (637–1248), coupled with low Y (1.06–1.48 ppm) and Yb (0.11–0.16 ppm) contents, as well as high Sr/Y (437–939 ppm) ratios, showing similar geochemical affinity to adakite

https://doi.org/10.5194/egusphere-2025-5595
Preprint. Discussion started: 23 January 2026

(Drummond and Defant, 1990). In the primitive mantle-normalized trace element pattern diagram, these samples are relatively enriched in large-ion lithophile elements (LILEs; e.g., Rb and Ba), but are relatively depleted in high field strength elements (HFSEs; e.g., Nb, Ta, and Ti) (Fig. 6b).

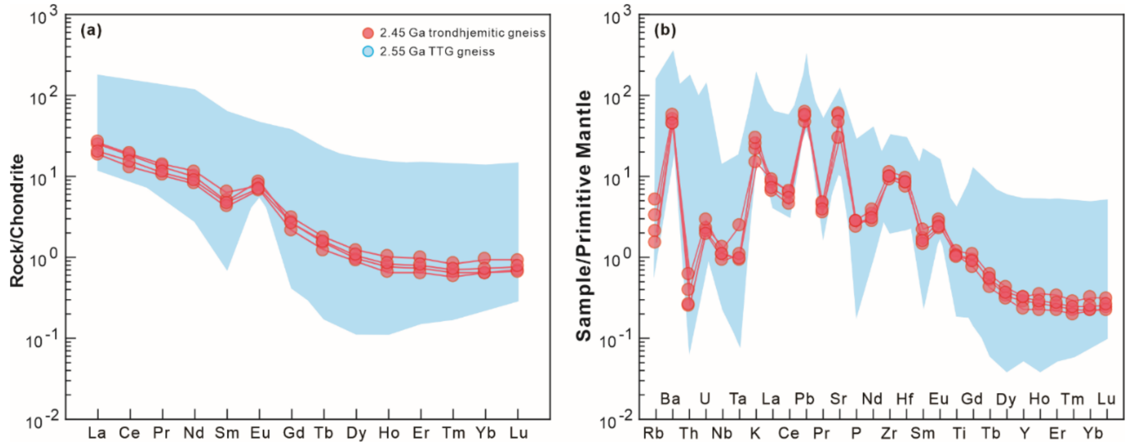

Figure 6: Chondrite-normalized REE patterns and primitive mantle-normalized trace elements spider diagrams for the trondhjemitic geniss samples (normalization values are from Sun and McDonough, 1989).

4.1 Zircon Hf-O isotopes

In situ zircon Hf-O isotope analyses results of sample 22ZH23-1 are presented in Supplementary Table S5. A total of 15 Lu-Hf isotope analyses show $^{176}Hf/^{177}Hf$ and $^{176}Lu/^{177}Hf$ ratios of 0.281338–0.281379 and 0.000444–0.001004, respectively. They have concentrated $\varepsilon_{Hf}(t)$ values of +3.3 to +4.9, with corresponding T_{DM2} ages varying from 2671 to 2769 Ma (Fig. 7a). Fifteen O isotopic analyses from this sample yield $\delta^{18}O$ values of 5.96–6.53 ‰, which are higher than the range of mantle zircon (5.3‰ ± 0.6‰, 2σ; Valley, 2003) (Fig. 7b).

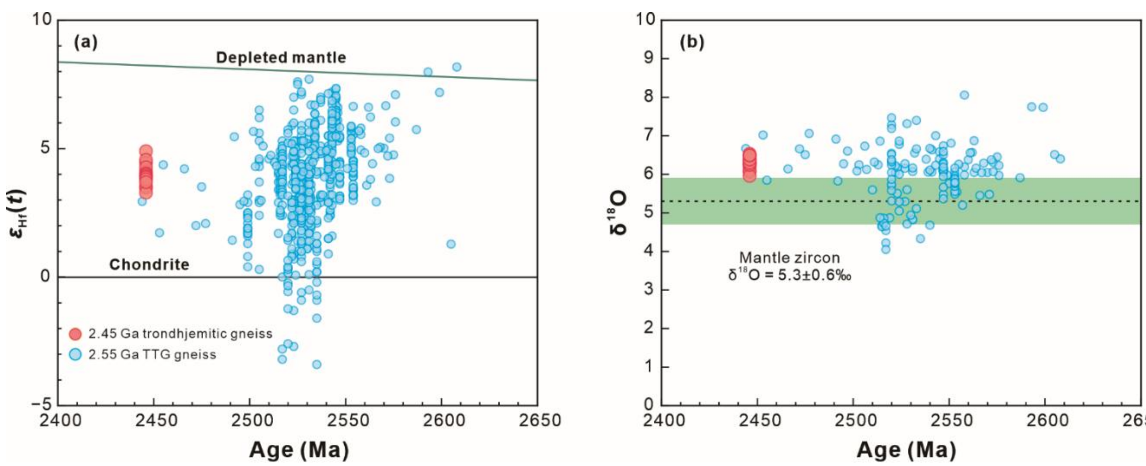

Figure 7: (a) Zircon $\varepsilon_{Hf}(t)$ vs. U-Pb age and (b) zircon $\delta^{18}O$ vs. U-Pb age diagrams of the trondhjemitic geniss samples. The data of the 2.55 Ga TTG gneiss are from Yang et al., 2008; Bai et al., 2014, 2016, 2019; Fu et al., 2016, 2019; Jing et al., 2025; Zhao et al., 2025a.

https://doi.org/10.5194/egusphere-2025-5595
Preprint. Discussion started: 23 January 2026

5 Discussion

5.1 Precambrian geochronological framework of Eastern Hebei

The geochronological framework in the region can be established by zircon U-Pb geochronological data from magmatic and metamorphic events. In this study, zircon U-Pb ages from the Qiuhuayu trondhjemitic gneiss yields two age populations with weighted mean ages of 2549 ± 29 Ma and 2446 ± 15 Ma, respectively. The older age is regarded as the crystallization age of inherited zircons, while the younger age represents the crystallization age of the protolith of this sample. This ca. 2.45 Ga trondhjemitic gneiss represents the first identification of early Paleoproterozoic (~2.45 Ga) magmatism in Eastern Hebei. In addition, a large number of late Neoarchean rocks (Geng et al., 2006; Yang et al., 2008; Zhang et al., 2012; Guo et al., 2013, 2014; 2015, 2017; Bai et al., 2014, 2016; Fu et al., 2016; Yao et al., 2017; Li et al., 2019; Wang et al., 2019 a, b, c; Duan et al., 2022) and sporadic Eoarchean to Mesoarchean rocks (Nutman et al., 2011; Sun et al., 2016; Liou et al., 2019; Wan et al, 2021, 2023; Dong et al., 2024, 2025; Zhao et al., 2025b) have also been reported in Eastern Hebei. We summarize the published zircon U-Pb age data from the magmatic rocks in Eastern Hebei. Ages with a concordance of < 95 % are excluded, and the remaining 2002 magmatic and 980 metamorphic zircon ages are used to establish the Precambrian geochronological framework of Eastern Hebei (Supplementary Table S1; Yang et al., 2008; Li et al., 2010, 2019; Nutman et al., 2011; Lv et al., 2012; Zhang et al., 2012; Guo et al., 2013, 2014, 2015, 2017; Bai et al., 2014, 2015, 2016, 2019; Han et al., 2014; Duan et al., 2015, 2022; Fu et al., 2016, 2017, 2019, 2021; Sun et al., 2016; Liou et al., 2019; Liou and Guo, 2019a; Lu et al., 2020; Wang et al., 2019 a, b, c; Wu et al., 2022; Dong et al., 2024, 2025; Zhao et al., 2025a, b). In combination with our new and collected age data, we identify four episodes of magmatic activities in Eastern Hebei: the Eoarchean (3.84–3.64 Ga), Paleoarchean (3.53–3.22 Ga), Mesoarchean (3.12–2.80 Ga), and late Neoarchean to early Paleoproterozoic (2.61–2.45 Ga) (Fig. 8a).

The Eoarchean (3.84–3.64 Ga) rocks in Eastern Hebei are primarily exposed in the Labashan area. The ~3.8 Ga granodioritic rock was first reported by Wan et al. (2021). Recently, the 3.84–3.75 Ga trondhjemitic gneiss, 3.79–3.77 Ga granodioritic gneiss, ~3.78 Ga quartz monzonite gneiss, and 3.79–3.64 Ga potassic granite gneiss have also been identified in the area (Dong et al., 2024). These rocks are in tectonic contact with the 3.4–3.1 Ga supracrustal rocks of the Labahsan Sequence, and both types of rock are hosted as enclaves in the 2.5 Ga potassic granite (Dong et al., 2024).

The Paleoarchean (3.53–3.22 Ga) rocks are mainly distributed in the Labashan, Longwan, and Huangbaiyu areas. The ~3.53 Ga trondhjemitic gneiss was discovered in the same location as the 3.8–3.6 Ga granitoid gneiss in the Labashan area (Zhao et al., 2025). The 3.51–3.38 Ga tonalitic, trondhjemitic, monzogranitic, and syenogranitic gneiss, with some meta-gabbro have also been reported in the Labashan area (Dong et al., 2025). The 3.45 Ga ultramafic-mafic suite was reported in the Longwan area and regarded as remnants of an enriched mantle plume (Wang et al., 2019a). The amphibolite and clinopyroxene-bearing hornblendite in the Huangbaiyu area yield Sm-Nd isochron ages of ~3.5 Ga (Huang et al., 1986; Jahn et al., 1987; Cui et al., 2018). However, these ages were challenged because some amphibolites occur as dykes intruding the ca. 2950 Ma rock (Nutman et al., 2011). In addition, the tonalitic gneiss with ages of 3.23–3.22 Ga have been identified in the Huangbaiyu area (Nutman et al., 2011).

https://doi.org/10.5194/egusphere-2025-5595
Preprint. Discussion started: 23 January 2026

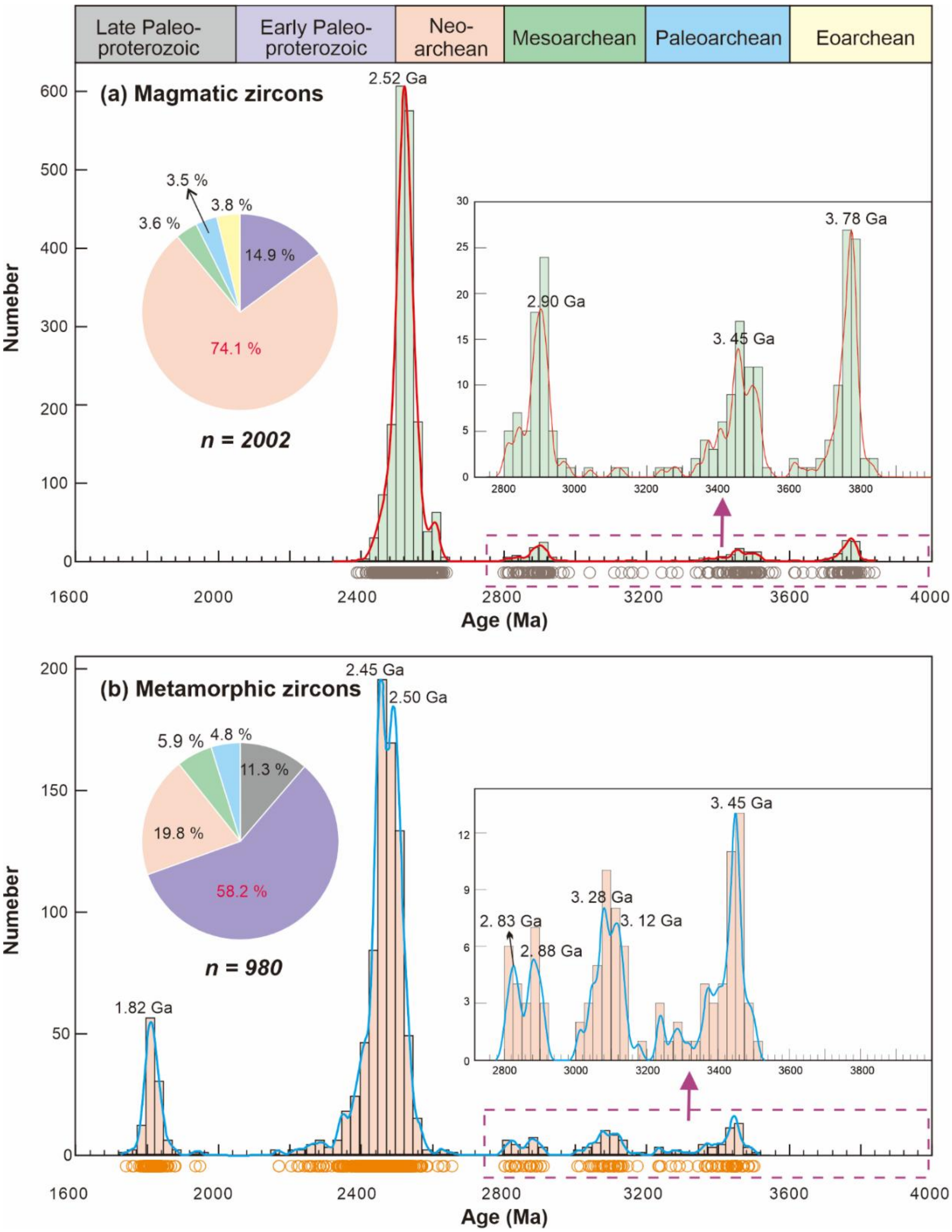

Figure 8: Histogram and kernel density estimation (KDE, Vermeesch, 2012) plots of the magmatic and metamorphic zircon ages from the Archean magmatic rocks in Eastern Hebei (Data from Yang et al., 2008; Li et al., 2010, 2019; Lv et al., 2012; Zhang et al., 2012; Guo et al., 2013, 2014, 2015, 2017; Bai et al., 2014, 2015, 2016, 2019; Han et al., 2014; Duan et al., 2015, 2022; Fu et al., 2016, 2017, 2019, 2021; Liou et al., 2019; Liou and Guo, 2019a; Lu et al., 2020; Wang et al., 2019 a, b, c; Wu et al., 2022; Dong et al., 2024, 2025; Zhao et al., 2025a, b).

The Mesoarchean (3.12–2.80 Ga) rocks are exposed in the Huangbaiyu, Labashan, and Caochang areas. Sun et al. (2016) reported ca. 3.1 Ga gneissic monzogranite and 3.0 Ga biotite plagioclase gneiss in the north of the Huangbaiyu area. Recent studies have revealed 3.12–2.96 Ga trondhjemitic gneiss, syenogranitic gneiss, and meta-gabbro in the Labashan area (Dong et al., 2025). The 2.90–2.80 Ga trondhjemitic, tonalitic, and dioritic gneiss have also been recognized in the Caochang area (Fu et al., 2019; Liou et al., 2019).

The late Neoarchean (2.61–2.49 Ga) rocks are widely distributed in Eastern Hebei and constitute the major part of the Precambrian basement in this area. It is composed mainly of TTG gneiss, dioritic gneiss, charnockite, potassic granite, and supracrustal rocks (Yang et al., 2008; Nutman et al., 2011; Bai et al., 2014, 2015, 2019; Duan et al., 2017, 2022; Fu et al., 2016, 2017; Li et al., 2024). These rocks show similar protolith magmatic ages of 2.61–2.49 Ga with a peak at ~2.52 Ga (Fig. 8a, Geng et al., 2006; Yang et al., 2008; Zhang et al., 2012; Guo et al., 2013, 2015, 2017; Bai et al., 2014, 2016, 2019; Fu et al., 2016; Yao et al., 2017; Li et al., 2019, 2024; Wang et al., 2019b, c; Duan et al., 2022). The ~2.45 Ga trondhjemitic gneiss discovered in this study provides the first evidence for the early Paleoproterozoic magmatic activity in Eastern Hebei, suggesting that the late Neoarchean magmatism persisted into the early Paleoproterozoic (~2.45 Ga).It is noteworthy that the basement of Eastern Hebei experienced intensive metamorphism, as evidenced by a large number of metamorphic zircons from the Archean rocks in Eastern Hebei (Yang et al., 2008; Lv et al., 2012; Zhang et al., 2012; Guo et al., 2013, 2014, 2015, 2017; Bai et al., 2014, 2015, 2016, 2019; Duan et al., 2015, 2019; Fu et al., 2016, 2017, 2021; Li et al., 2019, 2024; Wang et al., 2019b, c; Lu et al., 2020). Based on a compilation of metamorphic zircon ages, five episodes of metamorphism are recognized, including the Paleoarchean (3.50–3.20 Ga), Mesoarchean (3.18–2.80 Ga), late Neoarchean (peat at ~2.50 Ga), early Paleoproterozoic (peat at ~2.45 Ga), and late Paleoproterozoic (~1.82 Ga) (Fig. 8b). The Paleoarchean and Mesoarchean metamorphism was primarily reported in the Labashan and Huangbaiyu areas (Wan et al., 2021; Dong et al., 2024, 2025; Zhao et al., 2025b). The late Neoarchean metamorphism is widespread and represents a major metamorphic event in Eastern Hebei (Guo et al., 2013, 2014, 2015, 2017; Bai et al., 2014, 2015, 2016, 2019; Duan et al., 2015, 2019; Fu et al., 2016, 2017, 2021; Yang et al., 2017a, b; Lu et al., 2020). The coexistence of ~2.45 Ga magmatism and peak metamorphism indicates the development of an early Paleoproterozoic tectonothermal event in Eastern Hebei (Bai et al., 2014, 2015, 2016, 2019; Wang et al., 2019b, c; Lu et al., 2020). Additionally, the late Paleoproterozoic (~1.81 Ga) metamorphism is locally recognized in the Saheqiao linear structural belt of Eastern Hebei and dominated by high-pressure granulite-facies metamorphism (Duan et al., 2015, 2019; Yang et al., 2017a, b).

In summary, four episodes of magmatic activities (3.84–3.64 Ga, 3.53–3.22 Ga, 3.12–2.80 Ga, and 2.61–2.45 Ga) and five episodes of metamorphism (3.50–3.23 Ga, 3.18–2.80 Ga, ~2.50 Ga, ~2.45 Ga, ~1.82 Ga) are identified in Eastern Hebei.

5.2 Petrogenesis of ~2.45 Ga trondhjemitic gneiss

For the TTG gneiss, it is essential to evaluate the impact of alteration and metamorphism on whole-rock geochemical composition. All samples show low loss on ignition (LOI = 0.40–0.73 wt.%) and negligible Ce anomalies (δCe = 0.93–1.01),

https://doi.org/10.5194/egusphere-2025-5595
Preprint. Discussion started: 23 January 2026

suggesting that their geochemical characteristics were not significantly changed by late metamorphism (Polat and Hofmann, 2003). Therefore, these geochemical data can be effectively used for petrogenetic interpretation.

Previous studies proposed that TTG rocks were derived from partial melting of hydrous basaltic rocks (Rapp and Watson, 1995; Rapp et al., 1999; Moyen, 2011; Moyen and Martin, 2012; Palin et al., 2016). However, some recent studies have emphasized the important role of amphibole and plagioclase fractional crystallization in the formation of TTG rocks (Liou and Guo, 2019b, 2022; Laurent et al., 2020). The highly and moderately incompatible elements exhibit different behaviors during partial melting and fractional crystallization processes, which can be used to distinguish these two processes (Schiano et al., 2010). In the La/Hf vs. La and Rb/Sr vs. Rb diagrams, the studied samples are distributed along the partial melting trends (Schiano et al., 2010, Fig. 9). Considering with the lack of coeval mafic rocks and cumulates in Eastern Hebei, we propose that the formation of the 2.45 Ga trondhjemitic gneiss was primarily controlled by the partial melting process (Martin et al., 2005; Macpherson et al., 2006).

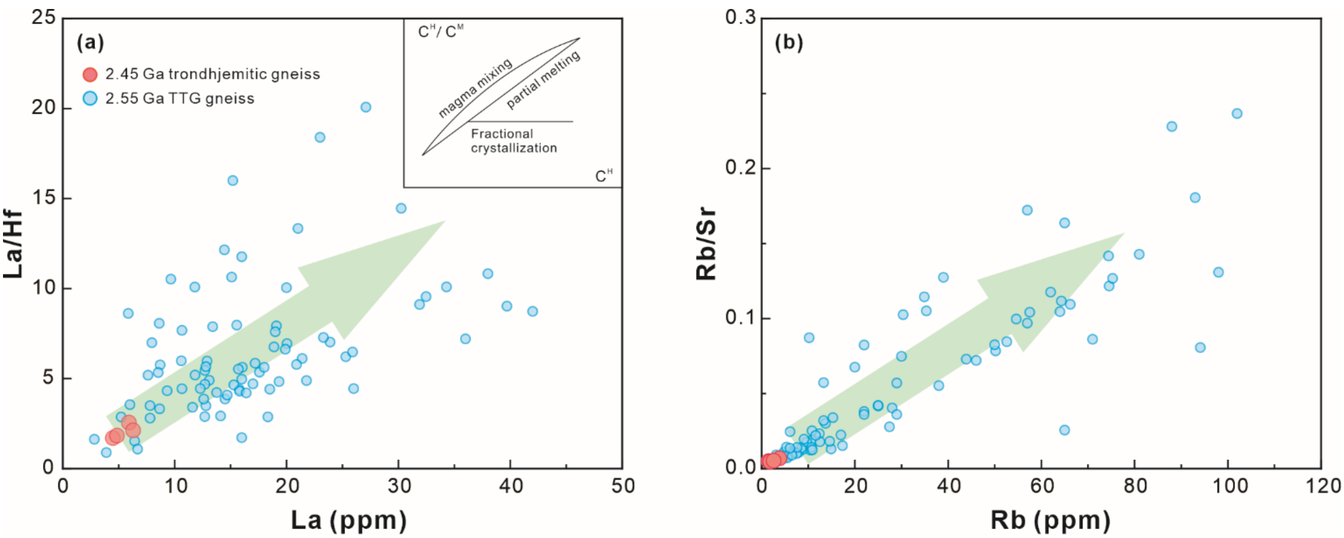

Figure 9: (a) La/Hf vs. La and (b) Rb/Sr vs. Rb diagrams. The inset is a schematic C^H/C^M vs. C^H plot, with superscripts H and M representing highly and moderately incompatible elements, respectively (after Schiano et al., 2010).

In this study, all samples show high Sr (637–1248 ppm) contents and Sr/Y (437–939 ppm) ratios, with low Y (1.06–1.48 ppm) and Yb (0.11–0.16 ppm) contents, akin to adakite (Drummond and Defant, 1990). They have high SiO_2 content (66.99–69.89 wt.%), low MgO (0.44–0.58 wt.%) and $Fe_2O_3^T$ (1.53–1.76 wt.%) contents, and $Mg^{\#}$ values (36–42), consistent with experimental partial melts from metabasaltic rocks, and belong to high-silica adakite (Fig. 10a, Rapp et al., 1999). In addition, these samples exhibit very low concentrations of Ni (2.82–5.13 ppm) and Cr (4.80–9.49 ppm), indicating that they originated from partial melting of a thickened lower crust (Fig. 10b, c; Rapp and Watson, 1995; Chung et al., 2003). In the Al_2O_3/(FeO^T+MgO)-(3CaO)-($5K_2O/Na_2O$) ternary diagram, all samples plot within the field of melts derived from low-K mafic rocks, implying the primary source of low-K mafic crust (Fig. 10d, Laurent et al., 2014). The trondhjemitic gneiss samples show positive zircon $\varepsilon_{Hf}(t)$ values (+3.3 to +4.9), further indicating a juvenile crust, which is also supported by their

https://doi.org/10.5194/egusphere-2025-5595
Preprint. Discussion started: 23 January 2026

higher zircon $\delta^{18}O$ values of 5.96–6.53 ‰ than mantle zircon ($\delta^{18}O_{Mantle} = 5.3 \pm 0.6$ ‰, Valley, 2003). Notably, a large number of the late Neoarchean (~2.55 Ga) TTG gneiss have been also reported in Eastern Hebei. Some of these rocks show comparable whole-rock geochemical and zircon Hf-O isotopic characteristics to the ~2.45 Ga TTG gneiss, characterized by high SiO_2, Al_2O_3, and Sr contents, low MgO, Y, Yb, Cr, and Ni contents, with positive zircon $\varepsilon_{Hf}(t)$ values and higher zircon $\delta^{18}O$ values than mantle zircon, supporting a magma source of the juvenile, low-K thickened lower crust (Figs. 5-7, 9-10: Rapp and Watson.1995; Rapp et al., 1999; Chung et al., 2003, Laurent et al., 2014).

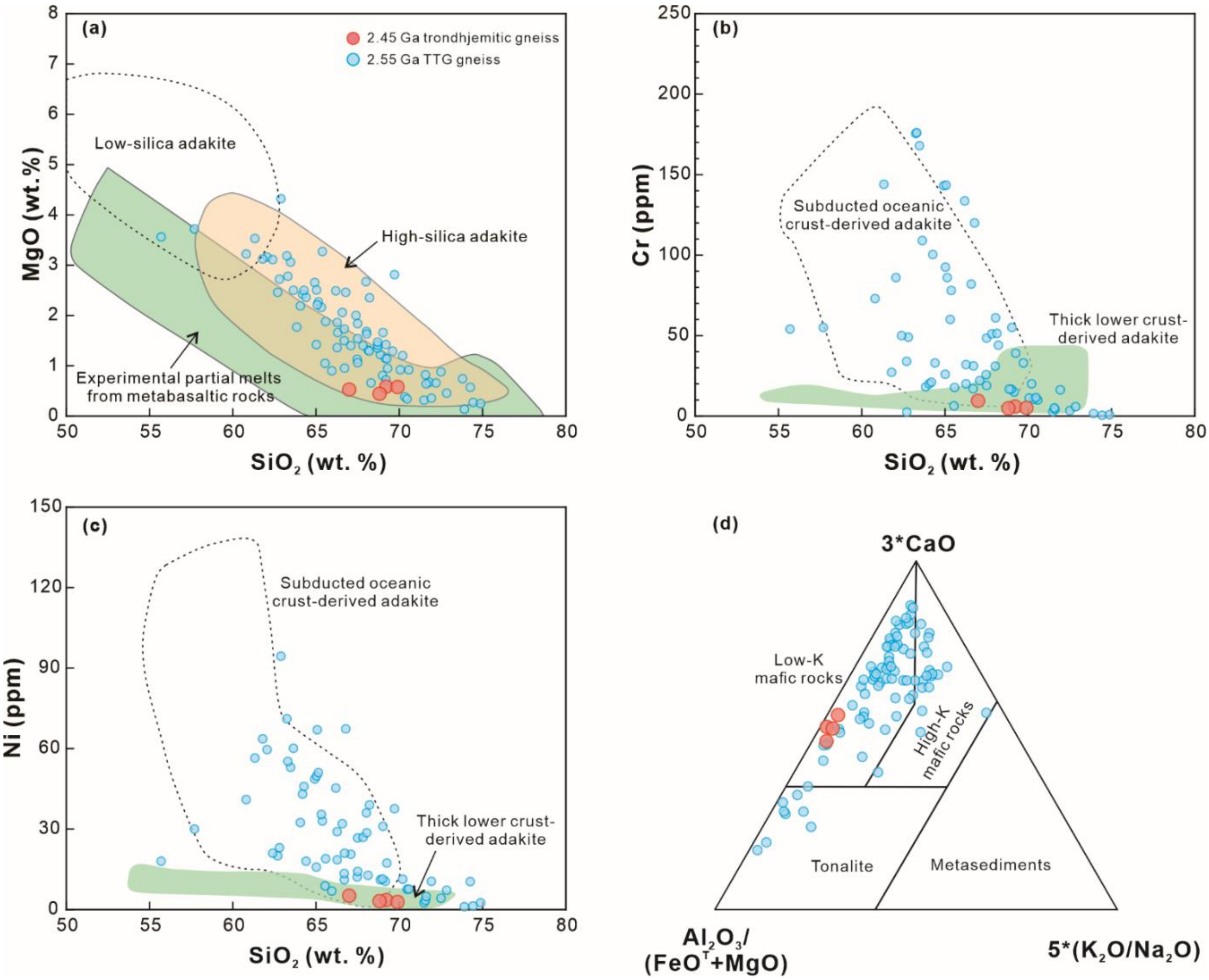

Figure 10: (a-c) Diagrams of MgO, Cr, and Ni versus SiO_2 (after Rapp and Watson, 1995; Rapp et al., 1999; Chung et al., 2003); (d) $Al_2O_3/(FeO^T+MgO)$–3*CaO–5*(K_2O/Na_2O) ternary diagram (after Laurent et al., 2014).

The 2.45 Ga trondhjemitic gneiss samples in this study are characterized by high Sr content, low Y, Yb, Nb, and Ta contents, as well as high Sr/Y, Nb/Ta, and $(La/Yb)_N$ ratios, implying that they formed under the high-pressure conditions, with garnet and rutile as the predominant residual phases (Fig. 11a, Martin et al., 1986; Defant and Drummond, 1990, Moyen, 2011; Qian and Hermann, 2013). Previous studies have revealed that garnet is compatible with HREEs (e.g., Yb) and Y (Rollinson,

https://doi.org/10.5194/egusphere-2025-5595
Preprint. Discussion started: 23 January 2026

1993; Taylor et al., 2015). Thus, the low Y and Yb contents, as well as high $(La/Yb)_N$ ratios of the studied samples, suggesting that garnet is the main residual mineral in the magma source. In addition, these samples show low concentrations of Ti, Nb, and Ta, coupled with their high Nb/Ta and low Nb/La ratios (Fig. 11b), indicating that the rutile was also residual, because rutile can control the contents of Ti, Nb, and Ta in the melt and increase the Nb/Ta ratios (Schmidt et al., 2004; Klemme et al., 2005; Xiong et al., 2006; John et al., 2011). Based on the high compatibility of Sr and Eu in plagioclase (Bédard, 2006), the high Sr content and significantly positive Eu anomalies of the 2.45 Ga trondhjemitic gneiss samples contradict residual plagioclase. Notably, our samples show extremely high Sr/Y values (637–1248), combined with their flat patterns of MREEs and HREEs, low $(Gd/Yb)_N$ values, and positive Eu anomalies (Fig. 6a), supporting that they have undergone amphibole fractional crystallization during the magma evolution (Tiepolo et al., 2007). The fractional crystallization of amphibole can also be revealed by the positive linear correlations in the Dy vs. Er (Fig. 11c, Drummond et al., 1996) and Ni vs. Cr diagrams (Fig. 11d, Rollinson, 1993).

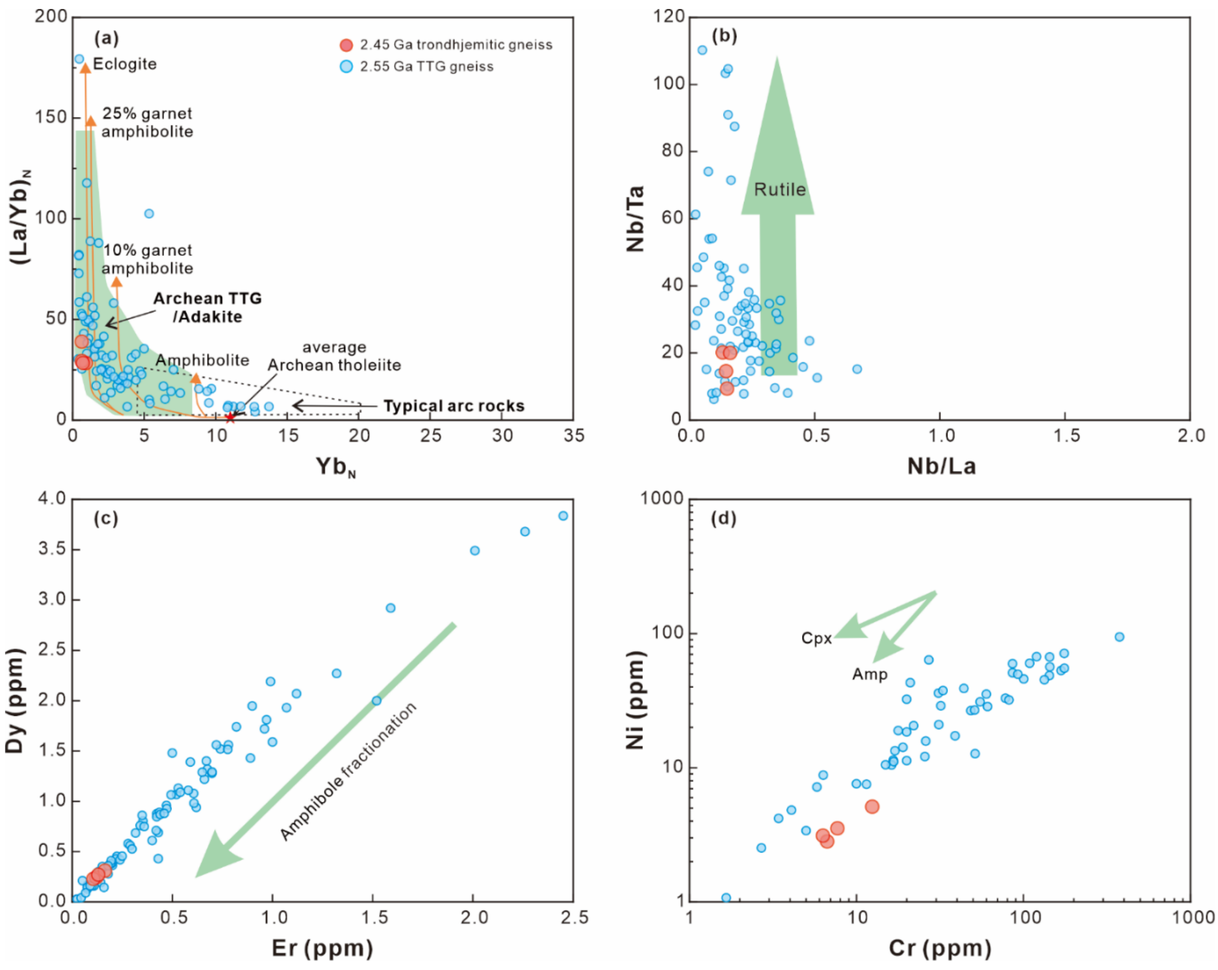

Figure 11: (a) $(La/Yb)_N$ vs. Yb_N diagram (after Martin, 1986); (b) Nb/Ta vs. Nb/La diagram (after Schmidt et al., 2004); (c) Dy vs. Er diagram (after Drummond et al., 1996); (d) Ni vs. Cr diagram (after Rollinson, 1993).

https://doi.org/10.5194/egusphere-2025-5595
Preprint. Discussion started: 23 January 2026

In summary, the protolith of the 2.45 Ga trondhjemitic gneiss in Eastern Hebei was probably derived from partial melting of a juvenile, low-K thickened lower crust, with garnet and rutile as residues. They have undergone amphibole fractional crystallization during magma evolution.

5.3 Eoarchean to early Paleoproterozoic crustal evolution in Eastern Hebei

The growth and reworking of continental crust have been a topic of continued interest in Earth sciences (Belousova et al., 2010; Hawkesworth et al., 2010; Cawood et al., 2013; Spencer et al., 2017; Diwu et al., 2018, 2021, 2024). Continental crustal growth refers to the transfer of mantle-derived melts to the crust, leading to an increase in the total volume of newly generated (juvenile) crust (Belousova et al., 2010; Kemp and Hawkesworth, 2014; Dhuime et al., 2018; Diwu et al., 2024). In contrast, crustal reworking involves the recycling of pre-existing crust by magmatism, metamorphism, and sedimentation within the continental crust, with no change in the volume of the crust (Hawkesworth et al., 2010; Dhuime et al., 2018; Zhu et al., 2021). To constrain the timing of growth and reworking of continental crust, we have compiled 2002 published magmatic zircon U-Pb ages from Eastern Hebei, among which 1428 age data were coupled with Hf isotope data (Fig. 12, Yang et al., 2008; Li et al., 2010, 2019; Guo et al., 2013, 2014, 2015, 2017; Bai et al., 2014, 2015, 2016, 2019; Han et al., 2014; Fu et al., 2016, 2017, 2019, 2021; Liou et al., 2019; Liou and Guo, 2019a; Wang et al., 2019 a; Dong et al., 2024, 2025; Zhao et al., 2025a, b).

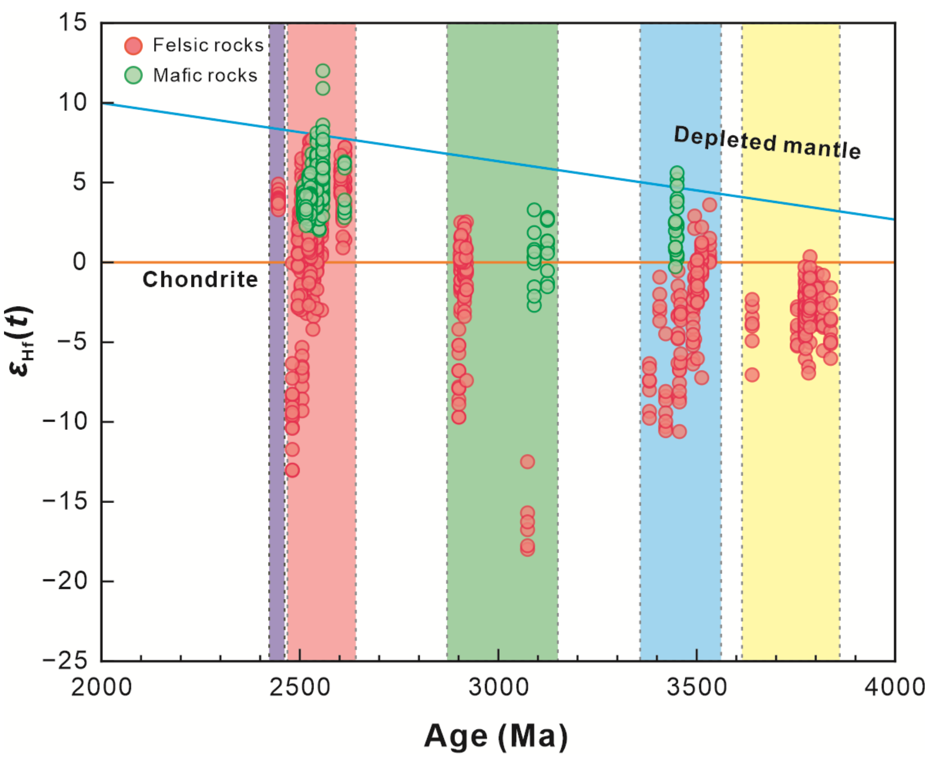

Figure 12: Magmatic zircon $\varepsilon_{Hf}(t)$ vs. U-Pb age of the magmatic rocks in Eastern Hebei (Data from Yang et al., 2008; Li et al., 2010, 2019; Guo et al., 2013, 2014, 2015, 2017; Bai et al., 2014, 2015, 2016, 2019; Han et al., 2014; Fu et al., 2016, 2017, 2019, 2021; Liou et al., 2019; Liou and Guo, 2019a; Wang et al., 2019 a; Dong et al., 2024, 2025; Zhao et al., 2025a, b). Bars in yellow, bule, green, red, and purple represent 3.86–3.64 Ga, 3.53–3.22 Ga, 3.12–2.80 Ga, 2.61–2.49 Ga, and 2.45 Ga.

https://doi.org/10.5194/egusphere-2025-5595
Preprint. Discussion started: 23 January 2026

Except for a single zircon with $\varepsilon_{Hf}(t)$ of 0.35, other 3.84–3.64 Ga magmatic zircons show negative $\varepsilon_{Hf}(t)$ values (-7.06 to -0.29) and T_{DM2} ages of 4.4–4.0 Ga (mainly 4.2–4.1 Ga), indicating that the Eoarchean rocks originated from the anatexis of older basaltic sources (Dong et al., 2024). However, no rocks older than 3.8 Ga were discovered in Eastern Hebei. In fact, the rocks with zircon T_{DM2} ages >4.0 Ga have also been reported in the Jack Hills, Acasta Gneiss complex, Qinling Orogenic Belt, Singhbhum Craton, and Kaapvaal Craton (Diwu et al., 2013; Kröner et al., 2014; Chaudhuri et al., 2018; Cavosie et al., 2019; Reimink et al., 2019), and were explained by partial melting of global mafic ultramafic crust from a magma ocean in early Earth (Kemp et al., 2010; Cawood et al., 2022; Wan et al., 2023). Thus, we propose that Eastern Hebei is dominated by Hadean crustal reworking in the Eoarchean.

The Paleoarchean (3.53–3.22 Ga) rocks contain various rock types of potassic granite, TTG gneiss, meta-gabbro, and meta-websterite. Nearly all potassic granites exhibit significantly negative zircon $\varepsilon_{Hf}(t)$ values of -10.55 to -0.18, with corresponding T_{DM2} ages of 4.37–3.78 Ga, indicating that they were derived from partial melting of ancient crust (Hadean to early Eoarchean). Magmatic zircons from the TTG gneiss have a wide range of $\varepsilon_{Hf}(t)$ values (-10.61 to 3.6, Dong et al., 2025; Zhao et al., 2025b), with majority (~80 %) of them yielding negative $\varepsilon_{Hf}(t)$ values (-10.61 to -0.2) and T_{DM2} ages of 4.50–3.80 Ga, suggesting that they originated from recycling of Eoarchean TTG rocks and Hadean mafic crust. The remaining magmatic zircons of the TTG gneiss show positive $\varepsilon_{Hf}(t)$ values of 3.6–0, implying a juvenile crust contribution. The 3.45 Ga meta-gabbro, with zircon $\varepsilon_{Hf}(t)$ of -0.28 to 2.56, was considered as a product of depleted mantle influenced by ancient crustal materials (Dong et al., 2025). The 3.45 Ga meta-websterite shows zircon $\varepsilon_{Hf}(t)$ of 5.6–0.2 and was regarded as remnants of an enriched mantle plume (Wang et al., 2019a). The occurrence of these 3.45 Ga Ga mantle-derived rocks indicates the generation of juvenile crust. Collectively, we suggest that Eastern Hebei is primarily characterized by crustal reworking with a minor contribution of crustal growth in the Paleoarchean.

The 3.07 Ga trondhjemitic gneiss in the Labashan area shows obviously negative zircon $\varepsilon_{Hf}(t)$ values of -17.99 to -12.50, with corresponding T_{DM2} ages of 4.55–4.21 Ga, suggesting that they originated from partial melting of Hadean mafic crust (Dong et al., 2025). In addition, the coeval mantle-derived meta-gabbro (3.12–3.09 Ga) has been recently reported in the same region, indicating the formation of juvenile crust (Dong et al., 2025). The ~2.9 Ga trondhjemitic gneiss in the Caozhuang area has negative zircon $\varepsilon_{Hf}(t)$ values (-9.7 to -4.2) and T_{DM2} ages of 3.89–3.61 Ga, indicating partial melting of the Eoarchean rocks (Fu et al., 2019). The 2.9–2.80 Ga dioritic gneiss and felsic orthogneiss in the Caochang area are characterized by a wide range of zircon $\varepsilon_{Hf}(t)$ values (-7.4 to 2.5), regarded as the result of mixing of mafic magma derived from a depleted mantle source and felsic magma from ancient crustal materials (Liou et al., 2019; Liou and Guo, 2019a). Therefore, we propose that both crustal growth and reworking occurred in the Mesoarchean (3.12–2.80 Ga) in Eastern Hebei. Notably, the proportion of the positive zircon $\varepsilon_{Hf}(t)$ values increased from 21% in the Paleoarchean to 43% in the Mesoarchean, attributable to enhanced crustal growth during this period (Fig. 12).

The late Neoarchean rocks (2.61–2.49 Ga) account for over 80 % of the Archean basement in Eastern Hebei (Yang et al., 2008; Nutman et al., 2011; Bai et al., 2014, 2015, 2019; Duan et al., 2017, 2022; Fu et al., 2016, 2017; Yao et al., 2017; Li et al., 2019, 2024; Wang et al., 2019b, c). Whether late Neoarchean magmatism represents significant crustal growth or reworking has long been controversial. Some researchers proposed that the late Neoarchean may represent a period of the 2.8–2.7 Ga crust reworking because the whole-rock Sm-Nd and zircon Lu-Hf model ages of the late Neoarchean magmatic zircons show a prominent age cluster centered on 2.8–2.7 Ga (Wu et al., 2005; Geng et al., 2012; Wan et al., 2022, 2024). However, the model age is a derivative parameter calculated based on several inherent assumptions (Hawkesworth et al., 2010; Fisher et al., 2014; Vervoort and Kemp, 2016; Diwu et al., 2024). The parameter variations tend to inevitably affect the model ages and propagate uncertainties more than 200–300 Ma (Kemp and Hawkesworth, 2014; Diwu et al., 2024). Thus, some scholars argued that the model ages should be used with caution when interpreting the generation of new crust (Diwu et al., 2012, 2024; Vervoort and Kemp, 2016). As shown in Fig. 12, the majority of the late Neoarchean magmatic rocks in Eastern Hebei have positive zircon $\varepsilon_{Hf}(t)$ values. Some of them are close to those of the contemporaneous depleted mantle (Fig. 7a), with their Hf model ages close to the corresponding U-Pb ages, supporting an origin from the juvenile crust. In addition, the late Neoarchean greenstone belts are widespread in Eastern Hebei, characterized by metamorphosed volcanic-sedimentary sequences, with the volume ratio of volcanics to sediments being ~3:1, and about 50 % of the volcanics are mafic (Shen et al., 1994; Guo et al., 2013, 2014, 2015, 2017; Fu et al., 2021). The meta-mafic rocks have MORB- or arc-like geochemical affinities involving a primary mantle source with minor continental crust contamination, indicating the growth of late Neoarchean juvenile crust in Eastern Hebei (Guo et al., 2013, 2014, 2015, 2017). Therefore, the late Neoarchean represents a major period of crustal growth in Eastern Hebei. Nevertheless, crustal reworking in the late Neoarchean cannot be completely ruled out, as part of the magmatic rocks have negative $\varepsilon_{Hf}(t)$ values and older Hf model ages, implying the partial melting of pre-existing crust (Fig. 8a). In addition, the K-rich granitoid rocks have been reported in Eastern Hebei, and were resulted from partial melting of the regionally widespread dioritic, granodioritic, monzonitic, and quartz monzonitic gneiss (Fu et al., 2017, 2019). Collectively, we propose that the late Neoarchean (2.61–2.49 Ga) is a major period of crustal growth in Eastern Hebei with a small portion of crustal reworking occurring.

This study first identified the 2.45 Ga trondjemitic gneiss in Eastern Hebei, which provides evidence for the magmatism during the TML in the Eastern Block, NCC. These rocks have concentrated, positive $\varepsilon_{Hf}(t)$ valuesfrom +3.3 to +4.9, with corresponding T_{DM2} ages varying from 2769 to 2671 Ma, suggesting the 2.45 Ga crustal growth in Eastern Hebei. Therefore, we propose that the early Paleoproterozoic era in the NCC was not a period of magmatic quiescence, and the plate tectonics and crustal growth remained active during this period. Notably, the 2.45 Ga trondjemitic gneiss shows similar whole-rock geochemical and zircon Hf-O isotopic characteristics to some 2.55 Ga TTG gneiss in Eastern Hebei (Figs. 4-7). Consequently, we suggest that the 2.45 Ga trondjemitic gneiss was probably a continuation of the late Neoarchean magmatism. In addition to the magmatic activity, some paleoclimatic changes also extensively occurred in the early Paleoproterozoic era. However, the relationship between magmatic activity and paleoclimatic upheavals needs further studies.

To sum up, we conclude that Eastern Hebei possesses a complex crustal evolution history from the Eoarchean to the early Paleoproterozoic. The Eoarchean (3.84–3.64 Ga) is characterized by Hadean crustal reworking. Both crustal growth and reworking occurred in the Paleoarchean (3.53–3.22 Ga), Mesoarchean (3.12–2.80 Ga), and late Neoarchean (2.61–2.49 Ga). Notably, the proportion of crustal growth increased from the Paleoarchean to the late Neoarchean, among which the late

https://doi.org/10.5194/egusphere-2025-5595
Preprint. Discussion started: 23 January 2026

Neoarchean represents a major period of crustal growth. The newly recognized ca. 2.45 Ga trondhjemitic gneiss was probably a continuation of the late Neoarchean magmatism, and the crustal growth persisted into this period.

6 Conclusions

(1) The 2.45 Ga trondhjemitic gneiss was discovered in Eastern Hebei, providing unambiguous evidence for an early Paleoproterozoic tectonothermal event in the Eastern Block, NCC.

(3) The protolith of the 2.45 Ga trondhjemitic gneiss was derived from partial melting of a juvenile, low-K thickened lower crust, with garnet and rutile as residues.

(2) Multiple stages of magmatism (3.84–3.64 Ga, 3.53–3.22 Ga, 3.12–2.80 Ga, and 2.61–2.45 Ga) and metamorphism (3.50–3.23 Ga, 3.18–2.80 Ga, ~2.50 Ga, ~2.45 Ga, ~1.82 Ga) are identified in Eastern Hebei.

(4) From the Eoarchean to the late Neoarchean, the crustal evolution of Eastern Hebei shifted from extensive reworking of ancient crust to a significant increase in crustal growth. The ca. 2.45 Ga trondhjemitic gneiss was probably a continuation of the late Neoarchean magmatism, and the crustal growth persisted into this period.

Data availability

Supplementary data to this article can be found online at xxx.

Author contributions

Jiahao Jing: Investigation, Validation, Formal analysis, Writing-Original draft preparation, Writing-Review & Editing, Visualization. Qian Liu: Investigation, Conceptualization, Methodology, Resources, Validation. Yigui Han: Validation. Jinlong Yao: Validation. Donghai Zhang: Validation. Chenyang Sun: Investigation, Methodology, Validation. Jiakang Zheng: Investigation. Guochun Zhao: Methodology, Validation.

Competing interest

The authors declare that they have no conflict of interest.

Acknowledgments

We are grateful to the staff from the Secondary Ion Mass Spectrometer Laboratory of Nanjing University for their assistance in the zircon O isotopic analyses. This work was financially supported by the National Key Research and Development Program of China (2024YFF0808000) and Northwest University Excellent Doctoral Thesis Cultivation Program (YB2024017).

References

Alkmim, F. F. and Teixeira, W.: The Paleoproterozoic Mineiro Belt and the Quadrilátero Ferrífero, in: São Francisco Craton, Eastern Brazil: Tectonic Genealogy of a Miniature Continent, edited by: Heilbron, M., Cordani, U. G., and Alkmim, F. F., Springer International Publishing, Cham, 71-94, 10.1007/978-3-319-01715-0_5, 2017.

Bai, W., Dong, C., Nutman, A. P., Xie, H., Liu, D., and Wan, Y.: Timing of late Neoarchean to late Paleoproterozoic events in the North China Craton: SHRIMP U-Pb dating and LA-ICP-MS Hf isotope analysis of zircons from magmatic and metamorphic rocks in the Santunying area, eastern Hebei, Gondwana Res., 76, 348-372, https://doi.org/10.1016/j.gr.2019.06.005, 2019.

Bai, X., Liu, S., Guo, R., Zhang, L., and Wang, W.: Zircon U–Pb–Hf isotopes and geochemistry of Neoarchean dioritic–trondhjemitic gneisses, Eastern Hebei, North China Craton: Constraints on petrogenesis and tectonic implications, Precambrian Res., 251, 1-20, https://doi.org/10.1016/j.precamres.2014.05.027, 2014.

Bai, X., Liu, S., Guo, R., and Wang, W.: Zircon U–Pb–Hf isotopes and geochemistry of two contrasting Neoarchean charnockitic rock series in Eastern Hebei, North China Craton: Implications for petrogenesis and tectonic setting, Precambrian Res., 267, 72-93, https://doi.org/10.1016/j.precamres.2015.06.004, 2015.

Bai, X., Liu, S., Guo, R., and Wang, W.: A Neoarchean arc–back-arc system in Eastern Hebei, North China Craton: Constraints from zircon U–Pb–Hf isotopes and geochemistry of dioritic–tonalitic–trondhjemitic–granodioritic (DTTG) gneisses and felsic paragneisses, Precambrian Res., 273, 90-111, https://doi.org/10.1016/j.precamres.2015.12.003, 2016.

Barker, F.: Chapter 1 - Trondhjemite: Definition, Environment and Hypotheses of Origin, in: Developments in Petrology, edited by: Barker, F., Elsevier, 1-12, https://doi.org/10.1016/B978-0-444-41765-7.50006-X, 1979.

Bédard, J. H.: A catalytic delamination-driven model for coupled genesis of Archaean crust and sub-continental lithospheric mantle, Geochim. Cosmochim. Ac., 70, 1188-1214, https://doi.org/10.1016/j.gca.2005.11.008, 2006.

Belousova, E. A., Kostitsyn, Y. A., Griffin, W. L., Begg, G. C., O'Reilly, S. Y., and Pearson, N. J.: The growth of the continental crust: Constraints from zircon Hf-isotope data, Lithos, 119, 457-466, https://doi.org/10.1016/j.lithos.2010.07.024, 2010.

Bouvier, A., Vervoort, J. D., and Patchett, P. J.: The Lu–Hf and Sm–Nd isotopic composition of CHUR: Constraints from unequilibrated chondrites and implications for the bulk composition of terrestrial planets, Earth Planet. Sci. Lett., 273, 48-57, https://doi.org/10.1016/j.epsl.2008.06.010, 2008.

Cavosie, A. J., Valley, J. W., and Wilde, S. A.: Chapter 12 - The Oldest Terrestrial Mineral Record: Thirty Years of Research on Hadean zircon from Jack Hills, Western Australia, in: Earth's Oldest Rocks (Second Edition), edited by: Van Kranendonk, M. J., Bennett, V. C., and Hoffmann, J. E., Elsevier, 255-278, https://doi.org/10.1016/B978-0-444-63901-1.00012-5, 2019.

Cawood, P. A., Hawkesworth, C. J., and Dhuime, B.: The continental record and the generation of continental crust, Geol. Soc. Am. Bull., 125, 14-32, 10.1130/b30722.1, 2013.

https://doi.org/10.5194/egusphere-2025-5595
Preprint. Discussion started: 23 January 2026

Cawood, P. A., Chowdhury, P., Mulder, J. A., Hawkesworth, C. J., Capitanio, F. A., Gunawardana, P. M., and Nebel, O.: Secular Evolution of Continents and the Earth System, Rev. Geophys., 60, e2022RG000789, https://doi.org/10.1029/2022RG000789, 2022.

Chaudhuri, T., Wan, Y., Mazumder, R., Ma, M., and Liu, D.: Evidence of Enriched, Hadean Mantle Reservoir from 4.2-4.0 Ga zircon xenocrysts from Paleoarchean TTGs of the Singhbhum Craton, Eastern India, Sci. Rep., 8, 7069, 10.1038/s41598-018-25494-6, 2018.

Condie, K. C., Belousova, E., Griffin, W. L., and Sircombe, K. N.: Granitoid events in space and time: Constraints from igneous and detrital zircon age spectra, Gondwana Res., 15, 228-242, https://doi.org/10.1016/j.gr.2008.06.001, 2009.

Chung, S.-L., Liu, D., Ji, J., Chu, M.-F., Lee, H.-Y., Wen, D.-J., Lo, C.-H., Lee, T.-Y., Qian, Q., and Zhang, Q.: Adakites from continental collision zones: Melting of thickened lower crust beneath southern Tibet, Geology, 31, 1021-1024, 10.1130/g19796.1, 2003.

Condie, K. C., Pisarevsky, S. A., Puetz, S. J., Spencer, C. J., Teixeira, W., and Meira Faleiros, F.: A reappraisal of the global tectono-magmatic lull at ~ 2.3 Ga, Precambrian Res., 376, 106690, https://doi.org/10.1016/j.precamres.2022.106690, 2022.

Davies, J. H. F. L. and Heaman, L. M.: New U–Pb baddeleyite and zircon ages for the Scourie dyke swarm: A long-lived large igneous province with implications for the Paleoproterozoic evolution of NW Scotland, Precambrian Res., 249, 180-198, https://doi.org/10.1016/j.precamres.2014.05.007, 2014.

Dhuime, B., Hawkesworth, C. J., Delavault, H., and Cawood, P. A.: Rates of generation and destruction of the continental crust: implications for continental growth, Philosophical Transactions of the Royal Society A: Mathematical, Physical and Engineering Sciences, 376, 20170403, doi:10.1098/rsta.2017.0403, 2018.

Diwu, C. R., Sun, Y., and Wang, Q.: The crustal growth and evolution of North China Craton: Revealed by Hf isotopes in detrital zircons from modern rivers, Acta Petrol. Sin., 28, 3520-3530, 2012 (in Chinese with English abstract).

Diwu, C. R, Liu, X., and Sun, Y.: The composition and evolution of the Taihua complex in the southern North China Craton, Acta Petrol. Sin., 34 (4), 999–1018, 2018 (in Chinese with English abstract).

Diwu, C. R.: Crustal growth and evolution of Archean continental crust in the southern North China Craton, Acta Petrol. Sin., 37 (2), 317-340, 2021 (in Chinese with English abstract).

Diwu, C. R., Sun, Y., Si, B. W., and Yan, M. J.: Archean continental crustal growth and reworking of the North China Craton: Constraints from zircon U-Pb age and Hf isotopic composition, Earth-Sci. Rev., 248, 104624, https://doi.org/10.1016/j.earscirev.2023.104624, 2024.

Dong, C., Liu, S., Nutman, A. P., Li, P., Xie, H., Li, Y., Liu, D., and Wan, Y.: New discovery of 3.84–3.64 Ga diverse granitoids in eastern Hebei, North China Craton: Petrogenesis and significance, Soc. Am. Bull., 136, 5249-5261, 10.1130/B37553.1, 2024.

Dong, C., Li, P., Nutman, A. P., Xie, H., Liu, S., Li, Y., Liu, D., and Wan, Y.: New discovery of Paleoarchean-Mesoarchean magmatic rocks in eastern Hebei, North China Craton: Petrogenesis and tectonic environment, Precambrian Res., 427, 107870, https://doi.org/10.1016/j.precamres.2025.107870, 2025.

Drummond, M. S., Defant, M. J., and Kepezhinskas, P. K.: Petrogenesis of slab-derived trondhjemite–tonalite–dacite/adakite magmas, Earth and Environmental Science Transactions of the Royal Society of Edinburgh, 87, 205-215, 10.1017/S0263593300006611, 1996.

Drummond, M. S. and Defant, M. J.: A model for Trondhjemite-Tonalite-Dacite Genesis and crustal growth via slab melting: Archean to modern comparisons, Journal of Geophysical Research: Solid Earth, 95, 21503-21521, https://doi.org/10.1029/JB095iB13p21503, 1990.

Du, L., Yang, C., Wyman, D. A., Nutman, A. P., Lu, Z., Song, H., Xie, H., Wan, Y., Zhao, L., Geng, Y., and Ren, L.: 2090–2070 Ma A-type granitoids in Zanhuang Complex: Further evidence on a Paleoproterozoic rift-related tectonic regime in the Trans-North China Orogen, Lithos, 254-255, 18-35, https://doi.org/10.1016/j.lithos.2016.03.007, 2016.

Duan, Q., Du, L., Song, H., Ren, L., Wyman, D. A., Geng, Y., Wang, J., and Yang, C.: Petrogenesis of the 2.3 Ga Lengkou metavolcanic rocks in the North China Craton: Implications for tectonic settings during the magmatic quiescence, Precambrian Res., 357, 106151, https://doi.org/10.1016/j.precamres.2021.106151, 2021.

Duan, Z., Wei, C., and Qian, J.: Metamorphic P–T paths and Zircon U–Pb age data for the Paleoproterozoic metabasic dykes of high-pressure granulite facies from Eastern Hebei, North China Craton, Precambrian Res., 271, 295-310, https://doi.org/10.1016/j.precamres.2015.10.015, 2015.

Duan, Z., Wei, C., and Rehman, H. U.: Metamorphic evolution and zircon ages of pelitic granulites in eastern Hebei, North China Craton: Insights into the regional Archean P–T–t history, Precambrian Res., 292, 240-257, https://doi.org/10.1016/j.precamres.2017.02.008, 2017.

Duan, Z., Wei, C., and Li, Z.: Metamorphic P–T paths and zircon u–pb ages of Paleoproterozoic metabasic dykes in eastern Hebei and northern Liaoning: Implications for the tectonic evolution of the North China Craton, Precambrian Res., 326, 124-141, https://doi.org/10.1016/j.precamres.2017.11.001, 2019.

Duan, Z., Wei, C., Li, Z., and Zhang, C.: Zircon U-Pb Dating and Metamorphism of Granitoid Gneisses and Supracrustal Rocks in Eastern Hebei, North China Craton, 12, 863, https://www.mdpi.com/2075-163X/12/7/863., 2022.

Eriksson, P. G. and Condie, K. C.: Cratonic sedimentation regimes in the ca. 2450–2000Ma period: Relationship to a possible widespread magmatic slowdown on Earth, Gondwana Res., 25, 30-47, https://doi.org/10.1016/j.gr.2012.08.005, 2014.

Fisher, C. M., Vervoort, J. D., and Hanchar, J. M.: Guidelines for reporting zircon Hf isotopic data by LA-MC-ICPMS and potential pitfalls in the interpretation of these data, Chem. Geol., 363, 125-133, https://doi.org/10.1016/j.chemgeo.2013.10.019, 2014.

French, J. E., Heaman, L. M., and Chacko, T.: Feasibility of chemical U–Th–total Pb baddeleyite dating by electron microprobe, Chem. Geol., 188, 85-104, https://doi.org/10.1016/S0009-2541(02)00074-8, 2002.

https://doi.org/10.5194/egusphere-2025-5595
Preprint. Discussion started: 23 January 2026

Fu, J., Liu, S., Chen, X., Bai, X., Guo, R., and Wang, W.: Petrogenesis of taxitic dioritic–tonalitic gneisses and Neoarchean crustal growth in Eastern Hebei, North China Craton, Precambrian Res., 284, 64-87, https://doi.org/10.1016/j.precamres.2016.08.002, 2016.

Fu, J., Liu, S., Wang, M., Chen, X., Guo, B., and Hu, F.: Late Neoarchean monzogranitic–syenogranitic gneisses in the Eastern Hebei–Western Liaoning Province, North China Craton: Petrogenesis and implications for tectonic setting, Precambrian Res., 303, 392-413, https://doi.org/10.1016/j.precamres.2017.05.002, 2017.

Fu, J., Liu, S., Zhang, B., Guo, R., and Wang, M.: A Neoarchean K-rich granitoid belt in the northern North China Craton, Precambrian Res., 328, 193-216, https://doi.org/10.1016/j.precamres.2019.04.021, 2019.

Fu, J., Liu, S., Sun, G., and Gao, L.: Two contrasting Neoarchean metavolcanic rock suites in eastern Hebei and their geodynamic implications for the northern North China Craton, Gondwana Res., 95, 45-71, https://doi.org/10.1016/j.gr.2021.02.023, 2021.

Geng, Y.S., Liu, F.L., and Yang, C.H.: Magmatic event at the end of the Archean in Eastern Hebei Province and its geological implications, Acta Geol. Sin., 80, 819-833, 2006 (in Chinese with English abstract).

Geng, Y. S., Du, L., and Ren, L.: Growth and reworking of the early Precambrian continental crust in the North China Craton: Constraints from zircon Hf isotopes, Gondwana Res., 21, 517-529, https://doi.org/10.1016/j.gr.2011.07.006, 2012.

Griffin, W. L., Pearson, N. J., Belousova, E., Jackson, S. E., van Achterbergh, E., O'Reilly, S. Y., and Shee, S. R.: The Hf isotope composition of cratonic mantle: LAM-MC-ICPMS analysis of zircon megacrysts in kimberlites, Geochim. Cosmochim. Acta, 64, 133-147, https://doi.org/10.1016/S0016-7037(99)00343-9, 2000.

Griffin, W. L., Wang, X., Jackson, S. E., Pearson, N. J., O'Reilly, S. Y., Xu, X., and Zhou, X.: Zircon chemistry and magma mixing, SE China: In-situ analysis of Hf isotopes, Tonglu and Pingtan igneous complexes, Lithos, 61, 237-269, https://doi.org/10.1016/S0024-4937(02)00082-8, 2002.

Guo, R., Liu, S., Santosh, M., Li, Q., Bai, X., and Wang, W.: Geochemistry, zircon U–Pb geochronology and Lu–Hf isotopes of metavolcanics from eastern Hebei reveal Neoarchean subduction tectonics in the North China Craton, Gondwana Res., 24, 664-686, https://doi.org/10.1016/j.gr.2012.12.025, 2013.

Guo, R., Liu, S.W., Bai, X., Zhang, L.F., Wang, W., Hu, F.Y., and Yan, M.: Geochemistry and zircon U-Pb chronology of Shuangshanzi Group in the eastern Hebei province, North China Craton: constraints on petrogenesis and tectonic setting, Acta Petrol. Sin., 30, 2885-2904, 2014 (in Chinese with English abstract).

Guo, R., Liu, S., Wyman, D., Bai, X., Wang, W., Yan, M., and Li, Q.: Neoarchean subduction: A case study of arc volcanic rocks in Qinglong-Zhuzhangzi area of the Eastern Hebei Province, North China Craton, Precambrian Res., 264, 36-62, https://doi.org/10.1016/j.precamres.2015.04.007, 2015.

Guo, R., Liu, S., Bai, X., and Wang, W.: A Neoarchean subduction recorded by the Eastern Hebei Precambrian basement, North China Craton: Geochemical fingerprints from metavolcanic rocks of the Saheqiao-Shangying-Qinglong supracrustal belt, J. Asian Earth Sci., 135, 347-369, https://doi.org/10.1016/j.jseaes.2017.01.007, 2017.

https://doi.org/10.5194/egusphere-2025-5595
Preprint. Discussion started: 23 January 2026

Halls, H. C., Kumar, A., Srinivasan, R., and Hamilton, M. A.: Paleomagnetism and U–Pb geochronology of easterly trending dykes in the Dharwar craton, India: feldspar clouding, radiating dyke swarms and the position of India at 2.37Ga, Precambrian Res., 155, 47-68, https://doi.org/10.1016/j.precamres.2007.01.007, 2007.

Hartlaub, R. P., Heaman, L. M., Chacko, T., and Ashton, K. E.: Circa 2.3 Ga Magmatism of the Arrowsmith Orogeny, Uranium City Region, Western Churchill Craton, Canada, J Geol., 115, 181-195, 10.1086/510641, 2007.

Hawkesworth, C. J., Dhuime, B., Pietranik, A. B., Cawood, P. A., Kemp, A. I. S., and Storey, C. D.: The generation and evolution of the continental crust, J. Geol. Soc., 167, 229-248, 10.1144/0016-76492009-072, 2010.

Huang, X., Ziwei, B., and DePaolo, D. J.: Sm-Nd isotope study of early Archean rocks, Qianan, Hebei Province, China, Geochim. Cosmochim. Ac., 50, 625-631, https://doi.org/10.1016/0016-7037(86)90111-0, 1986.

Hu, Z., Li, X.-H., Luo, T., Zhang, W., Crowley, J., Li, Q., Ling, X., Yang, C., Li, Y., Feng, L., Xia, X., Zhang, S.-B., Wang, Z., Guo, J., Xu, L., Lin, J., Liu, X., Bao, Z., Liu, Y., Zong, K., Chen, W., and Hu, S.: Tanz zircon megacrysts: a new zircon reference material for the microbeam determination of U–Pb ages and Zr–O isotopes, J. Anal. Atom. Spectrom., 36, 2715-2734, 10.1039/D1JA00311A, 2021.

Jahn, B. M., Auvray, B., Cornichet, J., Bai, Y. L., Shen, Q. H., and Liu, D. Y.: 3.5 Ga old amphibolites from eastern Hebei Province, China: Field occurrence, petrography, Sm-Nd isochron age and REE geochemistry, Precambrian Res., 34, 311-346, https://doi.org/10.1016/0301-9268(87)90006-4, 1987.

Jing, J. H., Liu, Q., Han, Y. G., Yao, J. L., Zhang, D. H., Sun, C. Y., Wang, C., Zheng, J. K., Zhao, G. C.: Petrogenesis of Neoarchean tonalite-trondhjemite-granodiorite and dioritic gneisses in Eastern Hebei, North China: Implications for coexisting vertical and horizontal geodynamic regime, Geosci. Front., in press, 2025.

John, T., Klemd, R., Klemme, S., Pfänder, J. A., Elis Hoffmann, J., and Gao, J.: Nb–Ta fractionation by partial melting at the titanite–rutile transition, Contrib. Mineral. Petrol., 161, 35-45, 10.1007/s00410-010-0520-4, 2011.

Kemp, A. I. S., Wilde, S. A., Hawkesworth, C. J., Coath, C. D., Nemchin, A., Pidgeon, R. T., Vervoort, J. D., and DuFrane, S. A.: Hadean crustal evolution revisited: New constraints from Pb–Hf isotope systematics of the Jack Hills zircons, Earth Planet. Sci. Lett., 296, 45-56, https://doi.org/10.1016/j.epsl.2010.04.043, 2010.

Kemp, A. I. S. and Hawkesworth, C. J.: Growth and Differentiation of the Continental Crust from Isotope Studies of Accessory Minerals, in: Treatise on Geochemistry (Second Edition), edited by: Holland, H. D., and Turekian, K. K., Elsevier, Oxford, 379-421, https://doi.org/10.1016/B978-0-08-095975-7.00312-0, 2014.

Klemme, S., Prowatke, S., Hametner, K., and Günther, D.: Partitioning of trace elements between rutile and silicate melts: Implications for subduction zones, Geochim. Cosmochim. Ac., 69, 2361-2371, https://doi.org/10.1016/j.gca.2004.11.015, 2005.

Kröner, A., Hoffmann, J. E., Xie, H., Münker, C., Hegner, E., Wan, Y., Hofmann, A., Liu, D., and Yang, J.: Generation of early Archaean grey gneisses through melting of older crust in the eastern Kaapvaal craton, southern Africa, Precambrian Res., 255, 823-846, https://doi.org/10.1016/j.precamres.2014.07.017, 2014.

Kumar, A., Hamilton, M. A., and Halls, H. C.: A Paleoproterozoic giant radiating dyke swarm in the Dharwar Craton, southern India, Geochem. Geophys. Geosyst., 13, https://doi.org/10.1029/2011GC003926, 2012.

Laurent, O., Martin, H., Moyen, J. F., and Doucelance, R.: The diversity and evolution of late-Archean granitoids: Evidence for the onset of "modern-style" plate tectonics between 3.0 and 2.5Ga, Lithos, 205, 208-235, https://doi.org/10.1016/j.lithos.2014.06.012, 2014.

Laurent, O., Björnsen, J., Wotzlaw, J.-F., Bretscher, S., Pimenta Silva, M., Moyen, J.-F., Ulmer, P., and Bachmann, O.: Earth's earliest granitoids are crystal-rich magma reservoirs tapped by silicic eruptions, Nature Geosci., 13, 163-169, 10.1038/s41561-019-0520-6, 2020.

Li, T., Zhai, M., Peng, P., Chen, L., and Guo, J.: Ca. 2.5 billion year old coeval ultramafic–mafic and syenitic dykes in Eastern Hebei: Implications for cratonization of the North China Craton, Precambrian Res., 180, 143-155, https://doi.org/10.1016/j.precamres.2010.04.001, 2010.

Li, X. H., Long, W. G., Li, Q. L., Liu, Y., Zheng, Y. F., Yang, Y. H., Chamberlain, K. R., Wan, D. F., Guo, C. H., Wang, X. C., and Tao, H.: Penglai Zircon Megacrysts: A Potential New Working Reference Material for Microbeam Determination of Hf–O Isotopes and U–Pb Age, Geostand. Geoanal. Res., 34, 117-134, https://doi.org/10.1111/j.1751-908X.2010.00036.x, 2010.

Li, X. H., Tang, G., Gong, B., Yang, Y., Hou, K., Hu, Z., Li, Q., Liu, Y., and Li, W.: Qinghu zircon: A working reference for microbeam analysis of U-Pb age and Hf and O isotopes, Chin. Sci. Bull., 58, 4647-4654, 10.1007/s11434-013-5932-x, 2013.

Li, Z., Wei, C., Zhang, S., Yang, C., and Duan, Z.: Neoarchean granitoid gneisses in Eastern Hebei, North China Craton: Revisited, Precambrian Res., 324, 62-85, https://doi.org/10.1016/j.precamres.2019.01.020, 2019.

Li, Z., Wei, C., Yang, C., and Zhang, X.: A Deep Mantle Source for the Late Neoarchean Metamorphosed Basalts in Eastern Hebei, North China Craton: Insights from Whole-Rock Geochemistry and Sm-Nd Isotopes, and Zircon U-Pb-Hf Isotopes, J. Earth Sci-China., 35, 29-40, 10.1007/s12583-023-1807-5, 2024.

Liou, P. and Guo, J.: Deciphering the Mesoarchean to Neoarchean history of crustal growth and recycling in the Caochang region of the Eastern Hebei Province, North China Craton using combined zircon U–Pb and Lu-Hf isotope analysis, Lithos, 334-335, 281-294, https://doi.org/10.1016/j.lithos.2019.03.013, 2019a.

Liou, P. and Guo, J.: Generation of Archaean TTG Gneisses Through Amphibole-Dominated Fractionation, J. Geophys. Res. Solid Earth., 124, 3605-3619, https://doi.org/10.1029/2018JB017024, 2019b.

Liou, P., Guo, J., Huang, G., and Fan, W.: 2.9 Ga magmatism in Eastern Hebei, North China Craton, Precambrian Research, 326, 6-23, https://doi.org/10.1016/j.precamres.2017.11.002, 2019.

Liou, P., Wang, Z., Mitchell, R. N., Doucet, L. S., Li, M., Guo, J., and Zhai, M.: Fe isotopic evidence that "high pressure" TTGs formed at low pressure, Earth Planet. Sci. Lett., 592, 117645, https://doi.org/10.1016/j.epsl.2022.117645, 2022.

https://doi.org/10.5194/egusphere-2025-5595
Preprint. Discussion started: 23 January 2026

Liu, T. and Wei, C.: Metamorphic evolution of Archean ultrahigh-temperature mafic granulites from the western margin of Qian'an gneiss dome, eastern Hebei Province, North China Craton: Insights into the Archean tectonic regime, Precambrian Res., 318, 170-187, https://doi.org/10.1016/j.precamres.2018.10.007, 2018.

Liu, T. and Wei, C.: Metamorphic P–T paths and Zircon U–Pb ages of Archean ultra-high temperature paragneisses from the Qian'an gneiss dome, East Hebei terrane, North China Craton, J. Metamorph. Geol., 38, 329-356, https://doi.org/10.1111/jmg.12524, 2020.

Liu, T., Wei, C., Johnson, T. E., and Sizova, E.: Newly-discovered ultra-high temperature granulites from the East Hebei terrane, North China Craton, Sci. Bull., 67, 670-673, https://doi.org/10.1016/j.scib.2021.12.023, 2022.

Liu, Y., Hu, Z., Zong, K., Gao, C., Gao, S., Xu, J., and Chen, H.: Reappraisement and refinement of zircon U-Pb isotope and trace element analyses by LA-ICP-MS, Chin. Sci. Bull., 55, 1535-1546, 10.1007/s11434-010-3052-4, 2010.

Lu, H. and Wei, C.: Late Neoarchean or late Paleoproterozoic high-pressure granulite facies metamorphism from the East Hebei terrane, North China Craton, J. Asian Earth Sci., 190, 104195, https://doi.org/10.1016/j.jseaes.2019.104195, 2020.

Lu, J. S., Zhai, M. G., Lu, L. S., and Zhao, L.: P-T-t evolution of Neoarchaean to Paleoproterozoic pelitic granulites from the Jidong terrane, eastern North China Craton, Precambrian Res., 290, 1-15, https://doi.org/10.1016/j.precamres.2016.12.012, 2017.

Ludwig, K.R.: User's Manual for Isoplot 3.0: A Geochronological Toolkit for Microsoft Excel, special publication, 4, 1-71, 2003.

Lv, B., Zhai, M., Li, T., and Peng, P.: Zircon U–Pb ages and geochemistry of the Qinglong volcano-sedimentary rock series in Eastern Hebei: Implication for ~2500Ma intra-continental rifting in the North China Craton, Precambrian Res., 208-211, 145-160, https://doi.org/10.1016/j.precamres.2012.04.002, 2012.

Lyons, T. W., Reinhard, C. T., and Planavsky, N. J.: The rise of oxygen in Earth's early ocean and atmosphere, Nature, 506, 307-315, 10.1038/nature13068, 2014.

Macpherson, C. G., Dreher, S. T., and Thirlwall, M. F.: Adakites without slab melting: High pressure differentiation of island arc magma, Mindanao, the Philippines, Earth Planet. Sci. Lett., 243, 581-593, https://doi.org/10.1016/j.epsl.2005.12.034, 2006.

Maniar, P. D. and Piccoli, P. M.: Tectonic discrimination of granitoids, Geol. Soc. Am. Bull., 101, 635-643, 10.1130/0016-7606(1989)101<0635:Tdog>2.3.Co;2, 1989.

Martin, H., Smithies, R. H., Rapp, R., Moyen, J. F., and Champion, D.: An overview of adakite, tonalite–trondhjemite–granodiorite (TTG), and sanukitoid: relationships and some implications for crustal evolution, Lithos, 79, 1-24, https://doi.org/10.1016/j.lithos.2004.04.048, 2005.

Middlemost, E. A. K.: Naming materials in the magma/igneous rock system, Earth-Sci. Rev., 37, 215-224, https://doi.org/10.1016/0012-8252(94)90029-9, 1994.

Moyen, J. F., Martin, H., Jayananda, M., and Auvray, B.: Late Archaean granites: a typology based on the Dharwar Craton (India), Precambrian Res., 127, 103-123, https://doi.org/10.1016/S0301-9268(03)00183-9, 2003.

Moyen, J. F.: The composite Archaean grey gneisses: Petrological significance, and evidence for a non-unique tectonic setting for Archaean crustal growth, Lithos, 123, 21-36, https://doi.org/10.1016/j.lithos.2010.09.015, 2011.

Neil, B. J. C., Chacko, T., Heaman, L. M., Dufrane, S. A., Creaser, R. A., Martel, E., Canam, R., and Pearson, D. G.: 2.4–2.3 Ga granitoids of the Arrowsmith orogeny, southwestern Rae craton, Canada: Syn- and post-orogenic magmatism during a global tectono-magmatic lull, Precambrian Res., 427, 107880, https://doi.org/10.1016/j.precamres.2025.107880, 2025.

Nutman, A. P., Wan, Y., Du, L., Friend, C. R. L., Dong, C., Xie, H., Wang, W., Sun, H., and Liu, D.: Multistage late Neoarchaean crustal evolution of the North China Craton, eastern Hebei, Precambrian Res., 189, 43-65, https://doi.org/10.1016/j.precamres.2011.04.005, 2011.

O'Neill, C., Jellinek, A. M., and Lenardic, A.: Conditions for the onset of plate tectonics on terrestrial planets and moons, Earth Planet. Sci. Lett., 261, 20-32, https://doi.org/10.1016/j.epsl.2007.05.038, 2007.

Palin, R. M., Santosh, M., Cao, W., Li, S.-S., Hernández-Uribe, D., and Parsons, A.: Secular change and the onset of plate tectonics on Earth, Earth-Sci. Rev., 207, 103172, https://doi.org/10.1016/j.earscirev.2020.103172, 2020.

Peccerillo, A. and Taylor, S. R.: Geochemistry of eocene calc-alkaline volcanic rocks from the Kastamonu area, Northern Turkey, Contrib. Mineral. Petrol., 58, 63-81, 10.1007/BF00384745, 1976.

Pehrsson, S. J., Buchan, K. L., Eglington, B. M., Berman, R. M., and Rainbird, R. H.: Did plate tectonics shutdown in the Palaeoproterozoic? A view from the Siderian geologic record, Gondwana Res., 26, 803-815, https://doi.org/10.1016/j.gr.2014.06.001, 2014.

Polat, A. and Hofmann, A. W.: Alteration and geochemical patterns in the 3.7–3.8 Ga Isua greenstone belt, West Greenland, Precambrian Res., 126, 197-218, https://doi.org/10.1016/S0301-9268(03)00095-0, 2003.

Polat, A., Li, J., Fryer, B., Kusky, T., Gagnon, J., and Zhang, S.: Geochemical characteristics of the Neoarchean (2800–2700 Ma) Taishan greenstone belt, North China Craton: Evidence for plume–craton interaction, Chem. Geol., 230, 60-87, https://doi.org/10.1016/j.chemgeo.2005.11.012, 2006.

N. Ramesh, B., E, N., V, P., and M, V.: Preliminary anisotropy of magnetic susceptibility studies on 2367 Ma Bangalore-Karimnagar giant dyke swarm, southern India: Implications for magma flow, Phys. Earth Planet. In., 306, 106540, https://doi.org/10.1016/j.pepi.2020.106540, 2020.

Rapp, R. P. and Watson, E. B.: Dehydration Melting of Metabasalt at 8–32 kbar: Implications for Continental Growth and Crust-Mantle Recycling, J. Petrol., 36, 891-931, 10.1093/petrology/36.4.891, 1995.

Rapp, R. P., Shimizu, N., Norman, M. D., and Applegate, G. S.: Reaction between slab-derived melts and peridotite in the mantle wedge: experimental constraints at 3.8 GPa, Chem. Geol., 160, 335-356, https://doi.org/10.1016/S0009-2541(99)00106-0, 1999.

Rehman, H. U., Kitajima, K., Valley, J. W., Chung, S. L., Lee, H. Y., Yamamoto, H., and Khan, T.: Low-δ18O mantle-derived magma in Panjal Traps overprinted by hydrothermal alteration and Himalayan UHP metamorphism: Revealed by SIMS zircon analysis, Gondwana Res., 56, 12-22, https://doi.org/10.1016/j.gr.2017.12.004, 2018.

https://doi.org/10.5194/egusphere-2025-5595
Preprint. Discussion started: 23 January 2026

Reimink, J. R., Chacko, T., Stern, R. A., and Heaman, L. M.: Earth's earliest evolved crust generated in an Iceland-like setting, Nature Geosci., 7, 529-533, 10.1038/ngeo2170, 2014.

Rollinson, H.R.: Using Geochemical Data: Evaluation, Presentation, Longman Scientific and Technical, London, 52-61, https://doi.org/10.4324/9781315845548, 1993.

Schiano, P., Monzier, M., Eissen, J. P., Martin, H., and Koga, K. T.: Simple mixing as the major control of the evolution of volcanic suites in the Ecuadorian Andes, Contrib. Mineral. Petrol., 160, 297-312, 10.1007/s00410-009-0478-2, 2010.

Schmidt, M. W., Dardon, A., Chazot, G., and Vannucci, R.: The dependence of Nb and Ta rutile–melt partitioning on melt composition and Nb/Ta fractionation during subduction processes, Earth Planet. Sc. Lett., 226, 415-432, https://doi.org/10.1016/j.epsl.2004.08.010, 2004.

Shen, B. F., Luo, H., Li, S. B., Li, J. J., Peng, X. L., Hu, X. D., Mao, D. B., and Liang, R. X.: Geology and metallization of Archean greenstone belts in the North China Platform, Geological Publishing House, in Beijing, 1994 (in Chinese with English abstract).

Siégel, C., Schoneveld, L., Spaggiari, C., Le Vaillant, M., Barnes, S., Godel, B., Mahon, D., Verrall, M., Martin, L., Caruso, S., and Shelton, T.: A newly recognised mafic sill-hosted Ni-sulfide deposit emplaced during the 2.4 Ga Widgiemooltha dike swarm event, Eastern Goldfields, Western, AustraliaMiner. Deposita., 60, 653-676, 10.1007/s00126-024-01305-z, 2025.

Sláma, J., Košler, J., Condon, D. J., Crowley, J. L., Gerdes, A., Hanchar, J. M., Horstwood, M. S. A., Morris, G. A., Nasdala, L., Norberg, N., Schaltegger, U., Schoene, B., Tubrett, M. N., and Whitehouse, M. J.: Plešovice zircon–A new natural reference material for U–Pb and Hf isotopic microanalysis, Chem. Geol., 249, 1-35, https://doi.org/10.1016/j.chemgeo.2007.11.005, 2008.

Söderlund, U., Patchett, P. J., Vervoort, J. D., and Isachsen, C. E.: The 176Lu decay constant determined by Lu–Hf and U–Pb isotope systematics of Precambrian mafic intrusions, Earth Planet. Sci. Lett., 219, 311-324, https://doi.org/10.1016/S0012-821X(04)00012-3, 2004.

Söderlund, U., Bleeker, W., Demirer, K., Srivastava, R. K., Hamilton, M., Nilsson, M., Pesonen, L. J., Samal, A. K., Jayananda, M., Ernst, R. E., and Srinivas, M.: Emplacement ages of Paleoproterozoic mafic dyke swarms in eastern Dharwar craton, India: Implications for paleoreconstructions and support for a ~30° change in dyke trends from south to north, Precambrian Res., 329, 26-43, https://doi.org/10.1016/j.precamres.2018.12.017, 2019.

Spencer, C. J., Roberts, N. M. W., and Santosh, M.: Growth, destruction, and preservation of Earth's continental crust, Earth Sci. Rev, 172, 87-106, https://doi.org/10.1016/j.earscirev.2017.07.013, 2017.

Spencer, C. J., Murphy, J. B., Kirkland, C. L., Liu, Y., and Mitchell, R. N.: A Palaeoproterozoic tectono-magmatic lull as a potential trigger for the supercontinent cycle, Nature Geosci., 11, 97-101, 10.1038/s41561-017-0051-y, 2018.

Stepanova, A. V., Salnikova, E. B., Samsonov, A. V., Egorova, S. V., Larionova, Y. O., and Stepanov, V. S.: The 2.31Ga mafic dykes in the Karelian Craton, eastern Fennoscandian shield: U–Pb age, source characteristics and implications for continental break-up processes, Precambrian Res., 259, 43-57, https://doi.org/10.1016/j.precamres.2014.10.002, 2015.

Sun, S. S. and McDonough, W. F.: Chemical and isotopic systematics of oceanic basalts: implications for mantle composition and processes, Geological Society, London, Special Publications, 42, 313-345, doi:10.1144/GSL.SP.1989.042.01.19, 1989.

Sun, H. Y., Xie, H. Q., Liu, S. J., Dong, C. Y., Liu, D. Y., and Wan, Y. S.: Archean magmatism and metamorphism in the Huangbaiyu-Yangyashan area, eastern Hebei Province: evidence from SHRIMP zircon U-Pb dating, Geol. Bull. China, 35 (1), 27–42, 2016 (in Chinese with English abstract).

Taylor, R. J. M., Harley, S. L., Hinton, R. W., Elphick, S., Clark, C., and Kelly, N. M.: Experimental determination of REE partition coefficients between zircon, garnet and melt: a key to understanding high-T crustal processes, J. Metamorph. Geol., 33, 231-248, https://doi.org/10.1111/jmg.12118, 2015.

Teixeira, W., Ávila, C. A., Dussin, I. A., Corrêa Neto, A. V., Bongiolo, E. M., Santos, J. O., and Barbosa, N. S.: A juvenile accretion episode (2.35–2.32Ga) in the Mineiro belt and its role to the Minas accretionary orogeny: Zircon U–Pb–Hf and geochemical evidences, Precambrian Res., 256, 148-169, https://doi.org/10.1016/j.precamres.2014.11.009, 2015.

Tiepolo, M., Oberti, R., Zanetti, A., Vannucci, R., and Foley, S. F.: Trace-Element Partitioning Between Amphibole and Silicate Melt, Rev. Mineral. Geochem., 67, 417-452, 10.2138/rmg.2007.67.11, 2007.

Valley, J. W.: Oxygen Isotopes in Zircon, Rev. Mineral. Geochem., 53, 343-385, 10.2113/0530343, 2003.

Vermeesch, P.: On the visualisation of detrital age distributions, Chem. Geol., 312-313, 190-194, https://doi.org/10.1016/j.chemgeo.2012.04.021, 2012.

Vervoort, J. D. and Kemp, A. I. S.: Clarifying the zircon Hf isotope record of crust–mantle evolution, Chem. Geol., 425, 65-75, https://doi.org/10.1016/j.chemgeo.2016.01.023, 2016.

Wan, Y. S., Xie, H. Q., Wang, H. C., Li, P. C., Chu, H., Xiao, Z. B., Dong, C. Y., Liu, S. J., Li, Y., Hao, G. M., and Liu, D. Y.: Discovery of ~3.8 Ga TTG rocks in eastern Hebei, North China Craton, Acta Geol. Sin., 95 (5), 1321-1333, 2021 (in Chinese with English abstract).

Wan, Y. S., Dong, C. Y., Xie, H. Q., Li, Y., Wang, Y. Q., Wang, K. L.: Huge growth of the late Mesoarchean-early Neoarchean (2.6–3.0 Ga) continental crust in the North China Craton: a review, J. Geomech., 28, 866-906, 2022 (in Chinese with English abstract).

Wan, Y. S., Dong, C. Y., Xie, H. Q., Li, P. C., Liu, S. J., Wang, Y. Q., Wang, K. L., and Liu, D.Y.: Late Neoarchean magmatism in the North China Craton: Implication for tectonic regimes and cratonization, Earth Sci. Front., 31,01, 2024 (in Chinese with English abstract).

Wan, Y., Dong, C., Xie, H., Wilde, S. A., Liu, S., Li, P., Ma, M., Li, Y., Wang, Y., Wang, K., and Liu, D.: Hadean to early Mesoarchean rocks and zircons in the North China Craton: A review, Earth-Sci. Rev., 243, 104489, https://doi.org/10.1016/j.earscirev.2023.104489, 2023.

Wang, C., Song, S., Wei, C., Su, L., Allen, M. B., Niu, Y., Li, X.-H., and Dong, J.: Palaeoarchaean deep mantle heterogeneity recorded by enriched plume remnants, Nature Geosci., 12, 672-678, 10.1038/s41561-019-0410-y, 2019a.

https://doi.org/10.5194/egusphere-2025-5595
Preprint. Discussion started: 23 January 2026

Wang, J., Li, X., Ning, W., Kusky, T., Wang, L., Polat, A., and Deng, H.: Geology of a Neoarchean suture: Evidence from the Zunhua ophiolitic mélange of the Eastern Hebei Province, North China Craton, Geol. Soc. Am. Bull., 131, 1943-1964, 10.1130/b35138.1, 2019b.

Wang, J. and Long, X.: Early Paleoproterozoic TTG gneisses and potassic granitoids in the southern Trans-North China Orogen: Key constraints on the tectonic setting during the tectono-magmatic lull and the initiation of plate tectonics, Earth-Sci. Rev., 250, 104713, https://doi.org/10.1016/j.earscirev.2024.104713, 2024.

Wang, W., Liu, F. L., Ji, L., and Santosh, M.: Geochronology and geochemistry of the Neoarchean Lulong Complex in the eastern Hebei Province, North China Craton: Implications on regional crustal evolution, Precambrian Rese., 323, 102-125, https://doi.org/10.1016/j.precamres.2019.01.013, 2019c.

Wang, X., Huang, X. L., and Yang, F.: Geochronology and geochemistry of the Xiaoqinling Taihua Complex in the southern Trans-North China Orogen: Implications for magmatism during the early Paleoproterozoic global tectono-magmatic shutdown, Lithos, 402-403, 106248, https://doi.org/10.1016/j.lithos.2021.106248, 2021.

Wei, C.J.: Neoarchean granulite facies metamorphism and its tectonic implications from the East Hebei terrane, Acta Petrol. Sin., 34, 895–912, 2018 (in Chinese with English abstract).

Wiedenbeck, M., Allé, P., Corfu, F., Griffin, W. L., Meier, M., Oberli, F., Quadt, A. V., Roddick, J. C., And Spiegel, W.: Three natural zircon standards for U-Th-Pb, Lu-Hf, trace element, and REE analyses, Geostandards Newsletter, 19, 1-23, https://doi.org/10.1111/j.1751-908X.1995.tb00147.x, 1995.

Wingate, M.: Mafic dyke swarms and large igneous provinces in Western Australia get a digital makeover. Geol. Surv. Western Australia Rec. 2:4–8, 2017.

Wu, F. Y., Zhao, G. C., Wilde, S. A., and Sun, D. Y.: Nd isotopic constraints on crustal formation in the North China Craton, J. Asian Earth Sci., 24, 523-545, https://doi.org/10.1016/j.jseaes.2003.10.011, 2005.

Wu, Z., Wang, C., Song, S., Allen, M. B., Kusky, T., and Su, L.: Ultrahigh-pressure peridotites record Neoarchean collisional tectonics, Earth Planet. Sci. Lett., 596, 117787, https://doi.org/10.1016/j.epsl.2022.117787, 2022.

Xiong, X., Adam, J., Green, T. H., Niu, H., Wu, J., and Cai, Z.: Trace element characteristics of partial melts produced by melting of metabasalts at high pressures: Constraints on the formation condition of adakitic melts, Sci. China Earth Sci., 49, 915-925, 10.1007/s11430-006-0915-2, 2006.

Yang, C. and Wei, C.: Ultrahigh temperature (UHT) mafic granulites in the East Hebei, North China Craton: Constraints from a comparison between temperatures derived from REE-based thermometers and major element-based thermometers, Gondwana Res., 46, 156-169, https://doi.org/10.1016/j.gr.2017.02.017, 2017a.

Yang, C. and Wei, C.: Two phases of granulite facies metamorphism during the Neoarchean and Paleoproterozoic in the East Hebei, North China Craton: Records from mafic granulites, Precambrian Res., 301, 49-64, https://doi.org/10.1016/j.precamres.2017.09.005, 2017.

https://doi.org/10.5194/egusphere-2025-5595
Preprint. Discussion started: 23 January 2026

Yang, C. X., Santosh, M., Lloyd, J., Glorie, S., Anilkumar, Y., Anoop, K. S., Gao, P., and Kim, S.-W.: Breakup of the Neoarchean supercontinent Kenorland: Evidence from zircon and baddeleyite U-Pb ages of LIP-related mafic dykes in the Coorg Block, southern India, Geosci. Front., 15, 101804, https://doi.org/10.1016/j.gsf.2024.101804, 2024.

Yang, J. H., Wu, F. Y., Wilde, S. A., and Zhao, G.: Petrogenesis and geodynamics of Late Archean magmatism in eastern Hebei, eastern North China Craton: Geochronological, geochemical and Nd–Hf isotopic evidence, Precambrian Res., 167, 125-149, https://doi.org/10.1016/j.precamres.2008.07.004, 2008.

Yang, Q. Y. and Santosh, M.: Paleoproterozoic arc magmatism in the North China Craton: No Siderian global plate tectonic shutdown, Gondwana Res., 28, 82-105, https://doi.org/10.1016/j.gr.2014.08.005, 2015.

Yao, X. and Zhang, J.: A late Neoarchaean–early Palaeoproterozoic crustal thickening event in the eastern North China Craton: petrological and geochronological evidence from Eastern Hebei terrane, Int. Geol. Rev., 59, 502-522, 10.1080/00206814.2016.1233462, 2017.

Young, G. M.: Precambrian supercontinents, glaciations, atmospheric oxygenation, metazoan evolution and an impact that may have changed the second half of Earth history, Geosci. Front., 4, 247-261, https://doi.org/10.1016/j.gsf.2012.07.003, 2013.

Yuan, H. L., Gao, S., Dai, M. N., Zong, C.-L., Günther, D., Fontaine, G. H., Liu, X. M., and Diwu, C. R.: Simultaneous determinations of U–Pb age, Hf isotopes and trace element compositions of zircon by excimer laser-ablation quadrupole and multiple-collector ICP-MS, Chem. Geol., 247, 100-118, https://doi.org/10.1016/j.chemgeo.2007.10.003, 2008.

Zakharov, D. O., Bindeman, I. N., Serebryakov, N. S., Prave, A. R., Azimov, P. Y., and Babarina, I. I.: Low $\delta^{18}O$ rocks in the Belomorian belt, NW Russia, and Scourie dikes, NW Scotland: A record of ancient meteoric water captured by the early Paleoproterozoic global mafic magmatism, Precambrian Res., 333, 105431, https://doi.org/10.1016/j.precamres.2019.105431, 2019.

Zhai, M. G. and Peng, P.: Origin of early continents and beginning of plate tectonics, Sci. Bull. (Beijing), 65, 970-973, 10.1016/j.scib.2020.03.022, 2020.

Zhang, L., Zhai, M. G., Zhang, X., Xiang, P., Dai, Y., Wang, C., and Pirajno, F.: Formation age and tectonic setting of the Shirengou Neoarchean banded iron deposit in eastern Hebei Province: Constraints from geochemistry and SIMS zircon U–Pb dating, Precambrian Res., 222-223, 325-338, https://doi.org/10.1016/j.precamres.2011.09.007, 2012.

Zhao, C., Liu, J., Zhang, H., Zhang, C., Chen, J., Cui, D., and Zhang, J.: Low-pressure ~3.53 Ga trondhjemite in the Eastern Hebei: Implications on the continental nucleus formation of the North China Craton, Precambrian Res., 417, 107668, https://doi.org/10.1016/j.precamres.2024.107668, 2025b.

Zhao, C., Zhang, J., Zhao, G. C., Yin, C. Q., Chen, G., Liu, J., Liu, X., and Chen, W.: Kinematics and structural evolution of the Anziling dome-and-keel architecture in east China: Evidence of Neoarchean vertical tectonism in the North China Craton, Geol. Soc. Am. Bull., 134, 2115-2129, 10.1130/b36225.1, 2021.

https://doi.org/10.5194/egusphere-2025-5595
Preprint. Discussion started: 23 January 2026

Zhao, D. Y, Cawood, P. A., Teng, F.-Z., Zhao, G., Xia, X. P., Sun, M., and Wang, X.: A two-stage mantle plume-sagduction origin of Archean continental crust revealed by water and oxygen isotopes of TTGs, Sci. Adv., 11, eadr9513, 10.1126/sciadv.adr9513, 2025a.

Zhao, G. C., and Zhai, M. G.: Lithotectonic elements of Precambrian basement in the North China Craton: Review and tectonic implications, Gondwana Res., 23, 1207-1240, https://doi.org/10.1016/j.gr.2012.08.016, 2013.

Zhao, G. C., Sun, M., Wilde, S. A., and Li, S. Z.: Late Archean to Paleoproterozoic evolution of the North China Craton: key issues revisited, Precambrian Res., 136, 177-202, https://doi.org/10.1016/j.precamres.2004.10.002, 2005.

Zheng, Y., Zhou, Y., Zhai, M., Wang, X., Deng, X., Liu, R., Zhao, T., and Wu, T.: Ca. 2.1 Ga low-$\delta^{18}O$ gabbro-diorite association in southern North China Craton: Implications for an intraplate rifting, Lithos, 430-431, 106858, https://doi.org/10.1016/j.lithos.2022.106858, 2022.

Zhou, Y., Sun, Q., Zhao, T., and Zhai, M.: Petrogenesis of the early Paleoproterozoic low-$\delta^{18}O$ potassic granites in the southern NCC and its possible implications for no confluence of glaciations and magmatic shutdown at ca. 2.3 Ga, Precambrian Res., 361, 106258, https://doi.org/10.1016/j.precamres.2021.106258, 2021.

Zhou, Y. and Zhai, M.: Mantle plume-triggered rifting closely following Neoarchean cratonization revealed by 2.50–2.20 Ga magmatism across North China Craton, Earth-Sci. Rev, 230, 104060, https://doi.org/10.1016/j.earscirev.2022.104060, 2022.

Zhou, Y., Zhai, M., Mitchell, R. N., Cawood, P. A., Huang, G., Spencer, C. J., Chen, M., Li, Y., Zhao, T., and Wu, TLow $\delta^{18}O$ and $\delta^{30}Si$ TTG at ca. 2.3 Ga Hints at an Intraplate Rifting Onset of the Paleoproterozoic Supercontinent Cycle, J. Geophys. Res-Sol. Ea., 129, e2023JB027306, https://doi.org/10.1029/2023JB027306, 2024.

Zhu, R., Zhao, G., Xiao, W., Chen, L., and Tang, Y.: Origin, Accretion, and Reworking of Continents, Rev. Geophys., 59, e2019RG000689, https://doi.org/10.1029/2019RG000689, 2021.